

Contents lists available at [ScienceDirect](http://www.sciencedirect.com)

Journal of Quantitative Spectroscopy & Radiative Transfer

journal homepage: www.elsevier.com/locate/jqsrt

Optical tweezers: Theory and modelling



Timo A. Nieminen*, Nathaniel du Preez-Wilkinson, Alexander B. Stilgoe,
Vincent L.Y. Loke, Ann A.M. Bui, Halina Rubinsztein-Dunlop

The University of Queensland, Quantum Science Laboratory, School of Mathematics and Physics, Brisbane, QLD 4072, Australia

ARTICLE INFO

Article history:

Received 20 November 2013

Received in revised form

4 April 2014

Accepted 7 April 2014

Available online 13 April 2014

Keywords:

Optical tweezers

Laser trapping

Optical force

Optical torque

Light scattering

ABSTRACT

Since their development in the 1980s, optical tweezers have become a widely used and versatile tool in many fields. Outstanding applications include the quantitative measurement of forces in cell biology and biophysics. Computational modelling of optical tweezers is a valuable tool in support of experimental work, especially quantitative applications. We discuss the theory, and the theoretical and computational modelling of optical tweezers.

© 2014 Elsevier Ltd. All rights reserved.

1. Introduction

Before the 1970s, there seemed to be little, if any, prospect of terrestrial application of optical forces. That optical forces could be important in astronomical situations was known [79,143], because free from frictional forces, small accelerations could result in large changes in velocity over time, or in stellar atmospheres where irradiances could be extremely high. Indeed, detailed proposals for solar sail driven spacecraft had been made as early as 1924 [160]. However, the minuteness of optical forces appeared to condemn them to remain a subject for “heroic experiments” (such as the first experimental measurements by [95,123,124]). However, from the early 1970s onwards, optical forces proved capable of manipulating small objects, and two branches of technology developed: atom cooling and trapping, which led to Nobel Prize in Physics in 1997 [27,28,139] and 2001 [31,89], and optical tweezers, or the single-beam gradient trap, where a single tightly focussed

laser beam is used to three-dimensionally trap microscopic particles. Optical tweezers were immediately attractive in biological research, due to the ability to trap and move microorganisms without physical contact [13,176], which can even allow manipulation of organelles in live cells [76]. Further, the ability to measure small forces—from femto-newtons to some tens of piconewtons—has made optical tweezers a star player in quantitative biophysics and mechanobiology [120]. The original modern papers on optical forces [6] and optical tweezers [9] and historical perspectives by the pioneer of the field [7,8] provide a basis for a historical overview of the topic. In addition, there is a useful bibliography covering the first few decades of optical tweezers [92]. Since we are discussing the theory and modelling of optical tweezers, we can point out some interesting and useful early theoretical work. Roosen and Imbert [146], Roosen et al. [145], and Roosen [144] carried out early work (following Ashkin’s original experiments, but predating optical tweezers). Application of full-wave theories to modelling optical trapping closely followed the invention of optical tweezers; some key theoretical papers from the first decade of optical tweezers are by Barton et al. [11,12], Gussgard et al. [72], Visscher

* Corresponding author. Tel.: +61 7 3365 2422; fax: +61 7 3365 1242.
E-mail address: timo@physics.uq.edu.au (T.A. Nieminen).

and Brakenhoff [165,166], Wright et al. [173], and Ren et al. [142]. An interesting combination of theory and experiment is the early work using optical levitation to test scattering theory by Grehan and Gouesbet [68], Guilloateau et al. [70].

The chief difficulty in practical application of optical forces is that the ratio of momentum flux to energy flux is very small. These are related by the speed of light, such that the momentum flux p of a collimated beam, or ray of light, or plane wave, of power P is $p = nP/c$, where n is the refractive index, and c is the speed of light in free space. This means that the maximum force obtainable in air is less than 10 nN/W. Indeed, the lack of successful laboratory measurements until the beginning of the twentieth century made many skeptical of even the existence of such forces [44], despite earlier theoretical work suggesting their existence [41,14]. Early experimental efforts failed—John Michell demonstrated only the destruction of his experimental apparatus by concentrated sunlight [75] (this work was, however, very fruitful as it led to the development of the torsion balance), and the Crookes radiometer [33–35] demonstrated thermal, rather than optical, forces. Part of the difficulty was the lack of a complete theory of optics, until Maxwell's development of electromagnetic theory [110,111], with further clarification of the transport of momentum by electromagnetic fields and light following shortly [140,10,77]. Interestingly, the same result was obtained on thermodynamic grounds by Umov [161].

Even after the theoretical basis was known, and the first measurements had been made, practical applications appeared to be far-off, perhaps even infinitely far. Terrestrial application requires other forces such as gravity, friction, viscous drag, and Brownian motion to be overcome. For a 1 W beam to be able to lift a solid particle, it would need to be smaller than 100 μm in radius, for typical densities. This, in turn, requires the 1 W beam to be focussed to approximately the size of the particle, or smaller. In the absence of a coherent light source, the irradiance at the focal spot is limited by the *brightness theorem*—the irradiance at the focus cannot exceed the irradiance at the source, which follows from Liouville [97]. To achieve the required irradiance above, i.e., 1 W focussed into an area of 10^{-8} m^2 , would require a blackbody with a temperature of over 6000 K.

However, the development of the laser allowed these limits to the irradiance achievable by focussing light from extended sources to be overcome. Ashkin [7,8] realised that the laser enabled greater irradiances to be achieved, which should be sufficient to levitate small particles against gravity [6]. These traps were based on radiation pressure forces, where the beam pushes the particle in the direction of propagation. During these experiments, it was noticed that particles were trapped transversely within the beams—they were attracted to the regions of maximum electric field amplitude. These forces were manifestations of the *gradient force*, and Ashkin realised that it would be possible to produce a gradient force large enough to overcome the radiation pressure force (or *scattering force*), allowing three-dimensional trapping by a single laser beam [9]. The critical ingredient was tightly focussing the beam so that the field gradient is sufficiently large

in all directions from the focus. This requires a high-numerical aperture lens; a microscope objective is ideal, and a typical optical tweezers apparatus essentially consists of a laser beam focussed by a microscope, as shown in Fig. 1. The microscope objective conveniently allows the user to observe the trapped particle.

Once one accepts that light carries momentum, the existence of radiation pressure forces which push particles in the direction of propagation due to reflection or absorption follows naturally. The gradient force, which can act against the propagation of the beam, is more mysterious when first encountered. There are two simple qualitative explanations. The first is that the electric field of the beam induces a dipole moment in the trapped particle, which is then attracted to the region of highest field, in the same way as a steel ball bearing is attracted to a magnet. The second explanation is based on the momentum of a converging or diverging beam. The momentum of a converging or diverging beam is less than that of a collimated beam, since, for any part of the beam, only the component of the momentum parallel to the beam axis contributes to the total momentum. The more converging or diverging the beam, the lower the momentum, while the more collimated, the higher the momentum. Thus, if a trapped particle makes the beam more convergent or divergent, it reduces the momentum of the beam, and is pushed in the direction of propagation. If, on the other hand, it makes the beam more collimated, the force opposes the direction of propagation. A typical particle can be considered as a weak positive lens, and if the beam is converging (i.e., if the

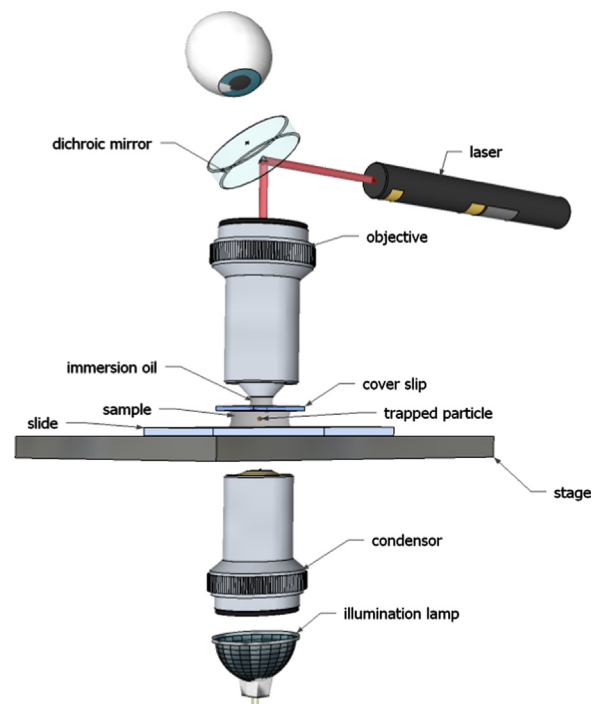


Fig. 1. A typical optical tweezers setup. A dichroic mirror in the microscope reflects incoming laser light towards the sample; and allows illumination light from the condenser to pass through to the eyepiece or camera. An oil layer is used between the lens and the cover slip, in order to allow for the use of numerical apertures greater than one.

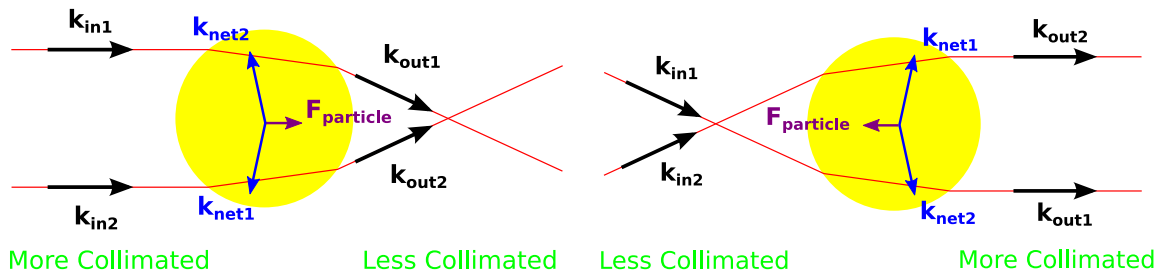


Fig. 2. Gradient force due to change of momentum of the beam. A trapped particle acts as a weak positive lens, and if before the focus (left), increases the convergence of the light, reducing its momentum. Due to the conservation of momentum, the rate of change of momentum of the two rays shown, plus the rate of change of momentum of the particle—the optical force acting on the particle—must equal zero. The resulting force pushes the particle towards the focus. If the particle is after the focus (right), the particle decreases the divergence of the beam, increasing its momentum. The resulting force pulls the particle towards the focus.

particle is before the focus), it will increase the convergence and be pushed towards the focus. If the beam is diverging (i.e., if the particle is past the focus), it will make the beam less divergent and be pulled towards the focus. This is illustrated in Fig. 2.

Both the gradient force and the scattering force, as the radiation pressure force is usually called in optical tweezers, result from the trapped particle changing the direction of the trapping beam—both result from scattering. This points towards a general method for calculating optical forces and the computational modelling of optical tweezers: optical tweezers as a scattering problem. Calculate the scattered field, and thus the total field, and therefrom determine the optical force.

In many ways, the scattering problem at the heart of optical tweezers is simple. Much of the complexity of the apparatus in Fig. 1 can be ignored—the viewing system and the collection and detection of the transmitted light do not affect the interaction between the trapping beam and particle, and the rest serves to deliver the trapping beam, suitably expanded to fill the back aperture of the objective. From the viewpoint of computational light scattering, optical tweezers consist of a particle interacting with a focussed beam. The particle is usually a single particle, and often sufficiently far from surfaces (such as the interface between the coverslip and the medium surrounding the particle) so that it can be treated as isolated. The speed of the particle, even if it is moving within the trap, is low enough so that the system can be treated as quasi-static. Since particle speeds will be very small compared to the speed of light, and the refractive index of the particle only changes slowly with frequency, Doppler shifts can be neglected. (This is unlike the case of atom trapping, where rapid change in the refractive index near resonance makes Doppler shifts an essential part of atom trapping and cooling. However, it can still be possible to study or measure Doppler shifts in order to obtain information about the motion of the particle.) Thus, we are left with the problem of elastic scattering of monochromatic coherent light. In addition, the particle of interest is often a homogeneous isotropic sphere.

On the other hand, the particles trapped in optical tweezers are typically both too large for small particle approximations such as Rayleigh scattering to be accurate, and too small for geometric optics to be accurate, requiring

the use of full-wave solutions. In addition, and perhaps a greater difficulty is that the incident light is a focussed beam, rather than the plane wave illumination common in scattering problems.

The theory and computational modelling of optical tweezers can be valuable tools. They can guide the development of new types of optical tweezers apparatus, and greatly aid the optimisation of existing methods (e.g., the optimisation of optically driven microrotors by [102]). When investigating new effects, modelling can indicate whether the major contributions to the observed effects have been identified (e.g., contributions of shape and material birefringence to the orientation of protein crystals in optical tweezers by [150]). Computational modelling can provide a versatile environment for performing simulated experiments free of experimental noise and providing access to quantities that cannot be measured easily, if at all. This can allow potential experimental discoveries to be predicted (e.g., the spinning of glass cylinders in circularly polarised light was predicted to be measurable, leading to experimental observation by [15], and the prediction of multiple equilibria from the interaction of multiple traps by [153]). New quantitative techniques can be developed where computational modelling plays a major role (e.g., the measurement of the refractive index of single microparticles by [91]).

2. General theory of optical tweezers

The main task when modelling optical tweezers is to calculate the force (and torque) exerted on the particle in the trap by the electromagnetic field as a function of its position (and orientation) within the trap. Often, the particle being considered is spherical and the torque is zero, and the orientation is irrelevant, reducing the problem to one of the optical forces as a function of position. The most important properties of the optical trap can be described by five quantities:

- The *trap strength*, which is the smallest maximum restoring force keeping the particle within the trap. This force is different in different directions from the equilibrium trapping position, and the particle is most likely to escape in the direction in which the maximum

force is weakest; therefore, we call this weakest maximum force the trap strength. This weakest force usually occurs along the beam axis in the direction of propagation (“downstream” along the beam), where the scattering force acts to push the particle out of the trap.

- The *radial trap strength*, which is the maximum restoring force acting to keep the particle within the trap against radial displacement from the equilibrium. Typically, this would be calculated for a purely radial displacement. However, the axial force is not usually zero during such a radial displacement, and the particle would not follow such a purely radial trajectory as it would be pushed up or down by the axial force [155]. Nonetheless, this straight-line radial trap strength provides a convenient estimate of the radial force required to remove a particle from the trap.
- The *equilibrium position*, which is the position where the optical force is zero, and the equilibrium is stable. Note that such an equilibrium position does not always exist, even if the particle can be trapped—for example, in Laguerre–Gauss beams, a small particle can be trapped in the ring-shaped beam, where it will orbit about the beam axis [45,129].
- The *radial spring constant*, which is the rate of increase of the restoring force with a change in the radial position. Usually, this will be determined from the equilibrium position as the starting point. In the vicinity of the equilibrium point, the trap can (usually) be approximately modelled as a linear spring, and the force given by

$$F_r = -k_r r. \quad (1)$$

The radial spring constant depends on the direction if the beam is not rotationally symmetric; the radial force can be different in the plane of polarisation and normal to the plane of polarisation, even for a Gaussian beam. Therefore, properly speaking, we should specify

the spring constant as a function of direction. For a Gaussian beam, it is sufficient to consider spring constants in the plane of polarisation, and normal to this plane. (This also applies to the radial trap strength.)

- The *axial spring constant*, which is the rate of increase of the restoring force with a change in the axial position. This is not as important as the radial spring constant, since it is less used for experimental measurements of force.

It is often useful to present these quantities as the dimensionless force and torque efficiencies, Q and τ , which can be converted to the force and torque by multiplying with nP/c , where n is the refractive index of the medium in which the particle is immersed, P is the beam power, and c is the speed of light in free space, to obtain the force, and P/ω , where ω is the optical frequency, to obtain the torque. The force efficiency can be considered as the force in units of nhk per photon, and the torque efficiency the torque in units of \hbar per photon. The relationship between these quantities and typical force–displacement curves is shown in Fig. 3.

These quantities are sufficient for many purposes for spherical particles. The (axial) trap strength, equilibrium position, and axial spring constant can typically be found with reasonable accuracy by calculating the axial force–displacement curve at 20–50 positions. The radial spring constant can then be found by one additional, off-axis, calculation (or two, if we are finding radial spring constants in two directions). The maximum radial force can be found by another 20–50 off-axis calculations. Therefore, there is clearly a need for repeated calculations for the same particle—the calculation of the optical force and torque at one point is rarely sufficient. For other purposes, it may be necessary to calculate the force field as a function of position in two or three dimensions. For a circularly polarised rotationally symmetric beam, the force

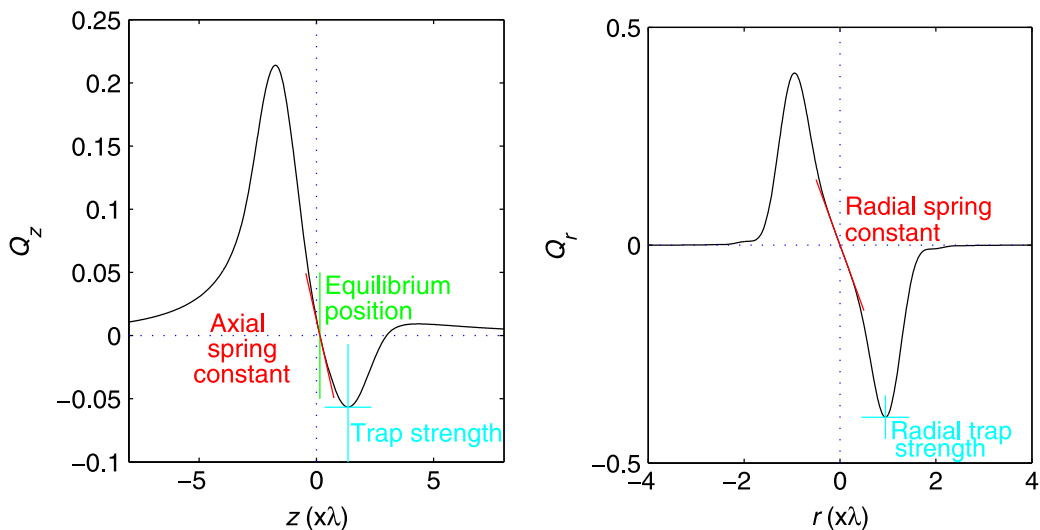


Fig. 3. Relationship between force–displacement curves and quantities describing an optical trap. (Left) Axial force versus axial displacement. (Right) Radial force versus radial displacement. The quantities of interest are the trap strength, the radial trap strength, the equilibrium position (the displacement at which the axial force is zero), the radial spring constant (the slope of the curve), and the axial spring constant (again, the slope of the curve).

field should also be rotationally symmetric, and it is sufficient to calculate the forces in a half plane out from the beam axis. In this case, a grid of approximately 30×30 points can be sufficient; based on practical experience, a grid much smaller than this either fails to sample the force field finely enough or to a large enough distance. Thus, about 1000 calculations of optical force are required. If we cannot assume an axisymmetric force field, and we wish to keep the same spatial resolution, then approximately 3×10^4 calculations are required. If repeated calculations can be performed quickly (e.g., faster than 1 s per position, or preferably faster than 0.1 s per position), calculation of the force field is feasible.

If non-spherical particles are considered, the number of degrees of freedom increases, by 2 for an axisymmetric particle, or 3 for a more general particle. Since this would increase the number of grid points by another factor of 1000 or 3×10^4 , if we were to maintain the same grid resolution, direct calculation of the force as a function of position and orientation over all combinations of position and orientation becomes impractical. The situation is even worse if we consider the trapping of multiple particles, where we will have 3 degrees of freedom per particle (or 5 or 6 if non-spherical).

One approach to such many-degree-of-freedom cases is to simulate the dynamics of the particle in the trap [22]. This requires calculation of non-optical forces as well. In particular, to calculate the motion of the particle requires modelling the interaction between the fluid and the particle. Typically, the Reynolds numbers for the fluid flow in such motion are very low (e.g., 10^{-3} – 10^{-6}), and the flow can be assumed to be perfectly laminar (Stokes flow or creeping flow). For spherical particles, one can simply assume that the drag is given by Stokes' law, with drag force $\mathbf{F}_{\text{drag}} = -6\pi\eta a\mathbf{v}$ for a particle of radius a moving at velocity \mathbf{v} through a medium of viscosity η . For simple shapes such as spheroids [30] and cylinders [46,3,43], suitable expressions for the translational and rotational drag coefficients are available. For complex shapes, such as some optically driven micromachines, direct numerical solution of the Laplace equation allows the flow field, and therefore the drag, to be found [4,5]. Including the viscous drag due to motion through the fluid is sufficient to determine the equilibrium position and orientation of a particle in a trap, by allowing it to “fall into” the trap [22]. The equilibrium can be found accurately even if the time step used as the particle approaches the equilibrium is quite large (resulting in large spatial steps), as long as small time steps are used in the vicinity of the equilibrium. Of course, the path the particle follows to the equilibrium will not necessarily be accurate, but this will not affect the determination of the equilibrium. Once the equilibrium position and orientation are found, translational and rotational spring constants can be found.

For a more realistic simulation of a particle in a trap, especially for small particles, it is necessary to include Brownian motion [21]. This can also be useful for finding equilibria as described above, preventing the particle becoming stuck in an unstable equilibrium.

A more difficult problem is modelling convective flow [109]. At the commonly used trapping wavelength

of 1064 nm, one can expect a temperature rise in the focal region of about 1 K per 100 mW of power [136]. The thermal expansion of the fluid will result in convective flow. This is a difficult problem because it involves flow in an open region, extending over a distance that is large compared to the size of the trapped particle, and usually with nearby surfaces affecting the flow (such as the microscope slide and cover slip). However, as far as free convection problems are concerned, it is a relatively simple problem—a convenient and accurate approximation is to assume that the temperature distribution is independent of the fluid flow. This results from the very short distances over which heat must travel, and consequent short times required, to reach very close to the equilibrium temperature distribution compared to the time required for the fluid to flow a significant distance [147]. Thus, one could determine the absorbed power density from the trapping beam, and then find the temperature distribution. From the temperature distribution, one then finds the variation in density (and viscosity, if needed or desired) of the fluid, and then the convective flow.

From this, we can see that calculating optical forces and torques is the main task when computationally modelling optical tweezers, but not the only task, and often not the most difficult task. Non-optical forces and torques due to viscous drag and Brownian motion need to be included for a complete model, with a major complication from the viscous drag due to convective flow past the particle. However, for many purposes, it is sufficient to calculate the optical force and torque only, or when orientation does not matter (such as for spherical particles), the optical force only.

Sometimes, we will want to calculate other quantities, even if these are not necessary for the calculation of optical forces or the dynamics of trapped particles. For example, we might wish to know the electric field, or the irradiance, or similar quantities. These can be of use to model observations of fluorescence, measurement of the transmitted beam [158], simply to investigate what is happening within the trap, or for visualisation.

There are two approaches we can take to calculate optical forces and torques. We can either calculate the force per unit volume acting on the particle within the trap or use conservation of momentum and the momentum flux towards the particle to determine the force. The former method is fundamentally a volume-based method, while the latter is a surface-based method. Both methods require knowledge of the electromagnetic field. We might expect a surface method to be more computationally efficient than a volume method, and this is often the case. However, in some circumstances, the volume-based method can be superior. Apart from possible computational advantages, the volume-based method can yield more information than the surface-based method: the internal stresses within the trapped object. If the trapped object is deformable, this might be essential information. Interestingly, both the volume and surface methods yield useful simple models for understanding the operation of optical tweezers in the small and large particle limits. We will discuss both methods below, and then consider efficient computational modelling of optical tweezers.

It is useful to introduce some common notation and terminology that will be used in the following sections. We will at different times consider both instantaneous electric and magnetic fields \mathbf{E} , \mathbf{D} , \mathbf{H} , and \mathbf{B} , which are real valued, and electric and magnetic field amplitudes \mathbf{E}_0 , \mathbf{D}_0 , \mathbf{H}_0 , and \mathbf{B}_0 , which are the complex-valued amplitudes of time-harmonic waves. The instantaneous fields and complex amplitudes for the E-field are related by

$$\mathbf{E} = \text{Re}\{\mathbf{E}_0 \exp(-i\omega t)\}, \quad (2)$$

with similar relationships for the other field quantities, and for other time-harmonic quantities, where ω is the angular frequency of the time-harmonic quantities.

We will characterise the electromagnetic properties of material media by the permittivity ϵ and permeability μ . Since we will consider non-magnetic dielectric materials, $\mu = \mu_0$, the permeability of free space. We can also describe the medium in terms of the refractive index $n = (\epsilon\mu/(\epsilon_0\mu_0))^{(1/2)} = (\epsilon/\epsilon_0)^{(1/2)}$, where ϵ_0 is the permittivity of free space, or the impedance $Z = (\mu/\epsilon)^{(1/2)}$. Note that $\mathbf{D} = \epsilon\mathbf{E} = \epsilon_0\mathbf{E} + \mathbf{P}$, where \mathbf{P} is the induced dielectric polarisation, or electric dipole moment per unit volume.

We will also separate the total field into incident and scattered parts where

$$\mathbf{E}^{(\text{total})} = \mathbf{E}^{(\text{inc})} + \mathbf{E}^{(\text{scattered})}. \quad (3)$$

Here, the incident field $\mathbf{E}^{(\text{inc})}$ is the field that would exist in the absence of the scattering particle, and the scattered field $\mathbf{E}^{(\text{scattered})}$ is the change in the field produced by the presence of the particle.

2.1. Force per unit volume, and the Rayleigh scattering approximation

Commonly, it is said that the force per unit volume exerted by electromagnetic fields on matter is given by the Lorentz force law:

$$\mathbf{f} = \rho\mathbf{E} + \mathbf{J} \times \mathbf{B}, \quad (4)$$

where the force density \mathbf{f} is given by the forces acting on the charge density ρ and the current density \mathbf{J} . However, a microscopic picture of uncharged dielectric matter suggests that this cannot be the correct force density. If we consider the simple case of a uniform sphere of such matter in an almost uniform electric field, the induced dipole moment per unit volume is almost constant—each molecule in the matter is polarised almost identically. Therefore, we expect an almost uniform force density. However, if we use the Lorentz force, and we replace the dielectric polarisation \mathbf{P} by the equivalent charge density $\rho = -\nabla \cdot \mathbf{P}$, we find that the force mostly acts on the boundaries of the polarised body. Since the force on a dipole in an electric field depends on the orientation of the dipole and the spatial derivative of the field parallel to the dipole in the direction of the dipole, the force density due to the electric field can be taken to be

$$\mathbf{f}_{\text{electric}} = (\mathbf{P} \cdot \nabla)\mathbf{E}. \quad (5)$$

If we also include the magnetic force acting on the polarisation current,

$$\mathbf{f}_{\text{magnetic}} = \frac{d\mathbf{P}}{dt} \times \mathbf{B}, \quad (6)$$

we can use the identity $(\mathbf{E} \cdot \nabla)\mathbf{E} = \nabla(\mathbf{E} \cdot \mathbf{E})/2 - \mathbf{E} \times (\nabla \times \mathbf{E})$, the relationship between \mathbf{P} and \mathbf{E} , and the Maxwell equations [48] to write the total force density as

$$\mathbf{f} = (\epsilon - \epsilon_0) \left(\frac{1}{2} \nabla(\mathbf{E} \cdot \mathbf{E}) + \frac{d}{dt}(\mathbf{E} \times \mathbf{B}) \right). \quad (7)$$

Since this force also acts on the surrounding medium, it is the excess force on the dielectric body that affects its motion, so the effective force density is

$$\mathbf{f} = (\epsilon_{\text{particle}} - \epsilon_{\text{medium}}) \left(\frac{1}{2} \nabla(\mathbf{E} \cdot \mathbf{E}) + \frac{d}{dt}(\mathbf{E} \times \mathbf{B}) \right). \quad (8)$$

While, in principle, we obtain the same total force on a dielectric body using either the Lorentz force or Eq. (8), the choice of force density can affect the accuracy of computational results. In particular, the equivalent surface charge on a dielectric particle in the trap may prove problematic. Other expressions for the force density are available [26,135], and it is worth exploring the diversity if planning a computational implementation of volume methods of calculating optical forces.

Other than the choice of force density, the computational implementation appears straightforward, except for the presence of derivatives in all of the different versions of the force density. A fine enough spatial grid for precise results can be computationally impractical in many cases, and lower precision may need to be accepted.

There is one case where this volume approach results in theoretically useful results and accurate numerical calculations: Rayleigh particles [74,24]. That is, particles that are much smaller than the wavelength. It is usual to consider a spherical particle, but the results are also applicable to non-spherical particles. We will consider a sphere, and afterward discuss the application to non-spherical particles.

For a sphere much smaller than the wavelength, the field is almost uniform through the volume of the sphere, and the force density is almost uniform. Thus, the volume integral of the force density is simple:

$$\mathbf{F} = \mathbf{f}V, \quad (9)$$

where $V = (4/3)\pi a^3$ is the volume of the sphere, and a is its radius. Therefore, we can express the total force in terms of a polarisability α :

$$\mathbf{F} = \alpha \left(\frac{1}{2} \nabla(\mathbf{E} \cdot \mathbf{E}) + \frac{d}{dt}(\mathbf{E} \times \mathbf{B}) \right). \quad (10)$$

The static polarisability of a sphere,

$$\alpha_{\text{static}} = 4\pi\epsilon_{\text{medium}}a^3 \left(\frac{\epsilon_{\text{particle}}/\epsilon_{\text{medium}} - 1}{2\epsilon_{\text{particle}}/\epsilon_{\text{medium}} + 1} \right), \quad (11)$$

is a good starting approximation for the polarisability α . If we assume that the incident field is time-harmonic, the time-averaged force is

$$\langle \mathbf{F} \rangle = \frac{1}{2} \text{Re} \left\{ \alpha \left(\frac{1}{2} \nabla(\mathbf{E}_0 \cdot \mathbf{E}_0^*) - 2i\omega \mathbf{E}_0 \times \mathbf{B}_0^* \right) \right\}. \quad (12)$$

The first term, proportional to the gradient of the irradiance, is the gradient force, and the second term, proportional to the Poynting vector, is the scattering force. A serious deficiency in the static polarisability for the time-harmonic polarisability is now apparent: the scattering force is zero if the polarisability is real, as the static polarisability is for a non-absorbing particle. Since a time-harmonic dipole with amplitude \mathbf{p}_0 radiates with average power $c^2 Z k^4 \mathbf{p}_0 \cdot \mathbf{p}_0^*/(12\pi)$, and the time-averaged rate of doing work on the dipole, $(1/2)\text{Re}(-i\omega \mathbf{p}_0 \cdot \mathbf{E}_0^*) = -(1/2)\text{Im}(\alpha) \mathbf{E}_0 \cdot \mathbf{E}_0^*$, is the source of this power, the imaginary component of the polarisability must be

$$\text{Im}(\alpha) = -\frac{cZk^3}{6\pi} |\alpha|^2. \quad (13)$$

This gives the required non-zero scattering force.

Noting that the real part of the polarisability is proportional to a^3 , or the volume of the particle, and, for a non-absorbing particle, the imaginary part is proportional to a^6 , or the volume squared, we can always obtain a scattering force smaller than the gradient force if we make the particle sufficiently small. Thus, materials that cannot be trapped for wavelength-sized particles can be trapped for very small particles; notable examples include gold nanoparticles [73]. Since Brownian motion will still act to remove the particle from the trap, it will provide a lower limit to the size of particle that can be trapped, unless Brownian motion is reduced, such as in optically trapped cold atoms. Since the gradient force dominates the transverse force in the vicinity of the equilibrium position, the radial spring constant will be proportional to a^3 .

Alas, the highly non-paraxial beams usually used for optical trapping do not have simple analytical expressions for the fields (unlike paraxial beams), and it is not possible to proceed further to analytical formulae for the gradient and scattering forces as functions of position within the beam.

2.2. Conservation of momentum, and the ray optics approximation

An alternative approach to finding the optical force exerted on a particle is to make use of conservation of momentum. The momentum flux through a surface can be found by integration of the Maxwell stress tensor \mathbf{T} , and the total force on bodies enclosed by the surface is

$$\mathbf{F} = \int_S \mathbf{T} \cdot d\mathbf{A} - \epsilon\mu \frac{d}{dt} \int_V \mathbf{S} dV. \quad (14)$$

The last term is required because the momentum that passes through the surface can be stored in the electromagnetic field within the enclosed volume, instead of being transferred to the enclosed bodies.

It is highly desirable to be able to ignore this last term, because if we must determine the fields throughout the enclosed volume in order to calculate it, we lose most of the computational advantages we might have gained from using a surface method. (Our only remaining advantage might be not necessary to calculate the spatial derivatives in Eq. (12).) Therefore, we ask: When can we ignore this volume term?

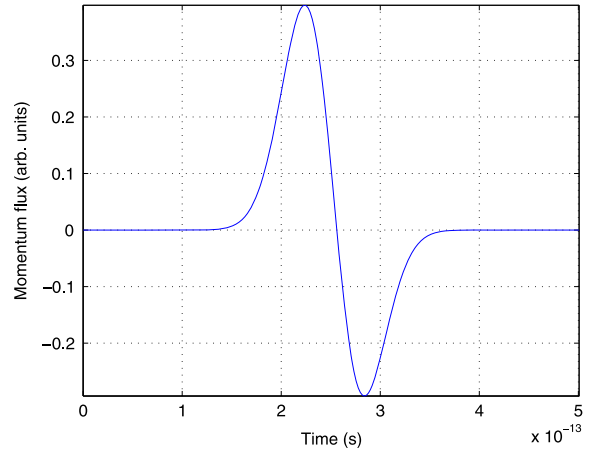


Fig. 4. The surface integral of the Maxwell stress tensor, $\int_S \mathbf{T} \cdot d\mathbf{A}$, over a surface around a spherical particle as a 100 fs pulse passes through the particle.

It is illuminating to calculate the momentum flux through a surface around a spherical particle due to the passage of a pulse of radiation. Such a calculation is shown in Fig. 4. The integrated momentum flux through the surface is dominated by the electromagnetic momentum temporarily residing in the enclosed volume; as the momentum enters, the integrated flux is positive, and as the momentum leaves, the flux is negative. This is a serious problem if we wish to know the instantaneous force acting on the particle—this would require the unwanted volume integral to determine the enclosed electromagnetic momentum. Worse, the force would be given by the difference between the flux and the rate of change of the enclosed momentum, and the errors in the flux and rate of change are likely to result in large relative errors in the force. It seems that, if we require the instantaneous force, integration of the force density over the volume of the particle is a better choice.

However, the instantaneous force is usually of little interest. Firstly, the typical trapping beam in optical tweezers is time-harmonic, and we are content with knowing the time-averaged force, since the variation of force over an optical cycle is too rapid to be measured—it is the time-averaged force that is responsible for observable effects. However, if we are using a time-domain method such as the finite-difference time-domain method (FDTD) to calculate the fields (often using a pulse for the purposes of obtaining the time-averaged force from what we can directly calculate: the instantaneous force. Secondly, even if we are interested in a pulsed beam in its own right, such as shown in Fig. 4, it is the impulse imparted to the particle by the pulse that is of interest, because, again, variation over the duration of the pulse will not be observed (unless the pulse is quite long, in which case it is possible to treat the pulse as a quasi-steady-state continuous wave: we can calculate the force due to a time-harmonic wave at the carrier frequency of the pulse, and simply modulate this by the pulse envelope). That is, it is the integral over time of the curve in Fig. 4 that we wish to calculate. (For a periodic

series of pulses, this is equivalent to calculating the time-averaged force.)

If we integrate Eq. (14) over time, from time t_1 to time t_2 , the impulse $\Delta \mathbf{p}$ delivered to the particle is

$$\Delta \mathbf{p} = \int_{t_1}^{t_2} \int_S \mathbf{T} \cdot d\mathbf{A} dt + \epsilon\mu \int_V \mathbf{S}(t_1) dV - \epsilon\mu \int_V \mathbf{S}(t_2) dV. \quad (15)$$

If we choose t_1 and t_2 so that the fields are identical at the two times, then the last two terms cancel, and it is not necessary to calculate any volume integrals. This condition is satisfied if we choose t_1 and t_2 to be one optical cycle apart for a continuous wave trapping beam, one pulse repetition period apart for a periodic series of pulses, or sufficiently before and after the pulse so that the fields are sufficiently close to zero for a single pulse. For a continuous wave, it will usually be possible to perform the time integral in Eq. (15) analytically, by replacing the instantaneous fields by the complex amplitudes and finding the time-average in the usual way. It is also a simple task to perform the time integration numerically, since the quantities being integrated are quadratic in the fields, and will vary as cosine squared, which can be integrated exactly with three intervals per optical cycle. In addition, even for a pulsed beam, the variation will be close enough to cosine squared for a three intervals per carrier optical cycle to give an accurate integral, unless the pulse is very short. Thus, for most practical purposes, it is sufficient to calculate the surface integral, without the volume integral.

At this point, it is useful to examine the convergence of this integral when performed numerically. The convergence as the spatial step size reduced is shown in Fig. 5, with relative errors at various step sizes given in Table 1. A step size of $\lambda/20$ results in a relative error of approximately 1%, and small step sizes give correspondingly small errors. Thus, direct numerical integration is a feasible approach, if moderate accuracy is sufficient.

It will be convenient to perform this integration in the far field. For a time-harmonic field, the conditions under which the volume terms in (15) cancel remain the same:

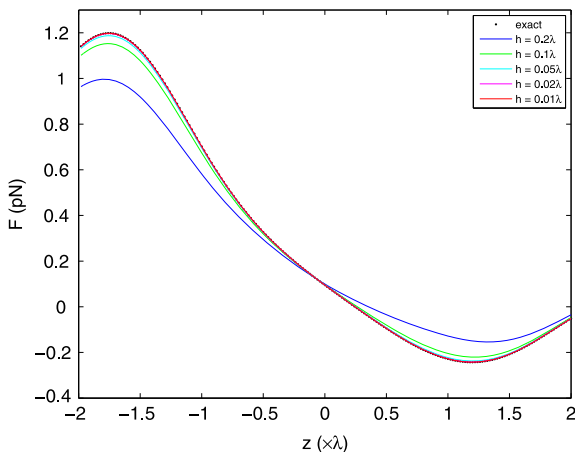


Fig. 5. Convergence of surface integral of the Maxwell stress tensor as point spacing is reduced. The relative errors are given in Table 1. The grid is a uniform angle polar and azimuthal grid; the grid spacing is the spacing in the polar direction, and the azimuthal spacing along the “equator”.

Table 1

Convergence of surface integral of the Maxwell stress tensor as point spacing is reduced. Curves of force as a function of position are shown in Fig. 5. The grid is a uniform angle polar and azimuthal grid; the grid spacing is the spacing in the polar direction, and the azimuthal spacing along the “equator”.

Step size h	Error
0.2λ	0.17
0.1λ	3.9×10^{-2}
0.05λ	9.6×10^{-3}
0.02λ	1.5×10^{-3}
0.01λ	3.8×10^{-4}

integrate over one optical cycle. This can provide some advantages. First, it allows this integration to be performed analytically in the T-matrix method, which will be described below. Second, since the field is a spherical wave in the far field, it can be represented by rays normal to a spherical surface in the far field. This allows simple calculation of the momentum flux in the geometric optics approximation.

The scattering force in the Rayleigh limit is often presented in terms of the conservation of momentum. If we assume that the incident field is an infinite plane wave, interference between the scattered field and the incident field can be ignored, except in the exact forward direction. The forward direction gives us the power—and therefore momentum—removed from the incident beam, and due to the symmetry of the scattered field, the scattered field transports a total momentum of zero. Thus, the scattering force can be written in terms of a radiation pressure cross section. While such a derivation of the scattering force depends on being able to neglect the effects of interference and independently calculate the momentum flux of the scattered field (which is zero) instead of having to calculate the momentum flux of the total outgoing field, the result is still useful for non-plane wave fields. Generally, the scattering force is given by the radiation pressure cross-section if, in the vicinity of the particle, the field appears like that of a plane wave. Apart from uniformity of the field, this also requires that \mathbf{E} and \mathbf{H} are in phase, which will be violated in the near field of other scattering objects. Therefore, the radiation pressure cross-section can be used for a single isolated particle, but not for particles near other scatterers. Not only is this important for closely spaced scatterers, it can also be important for calculating forces using the discrete-dipole approximation (DDA), where the scatterer is represented as a collection of closely packed dipole scatterers [23,24,80]. It is possible to extend the concept of cross-sections beyond the plane wave case [98,60,52], and thus extend the validity of cross-sections to particles large enough for the local field to appear non-plane wave.

2.3. Angular momentum

That electromagnetic waves carry angular momentum in addition to linear momentum should not be surprising; if a wave can exert a force, the moment of that force is a torque. Just as force is a transfer of momentum, torque is a

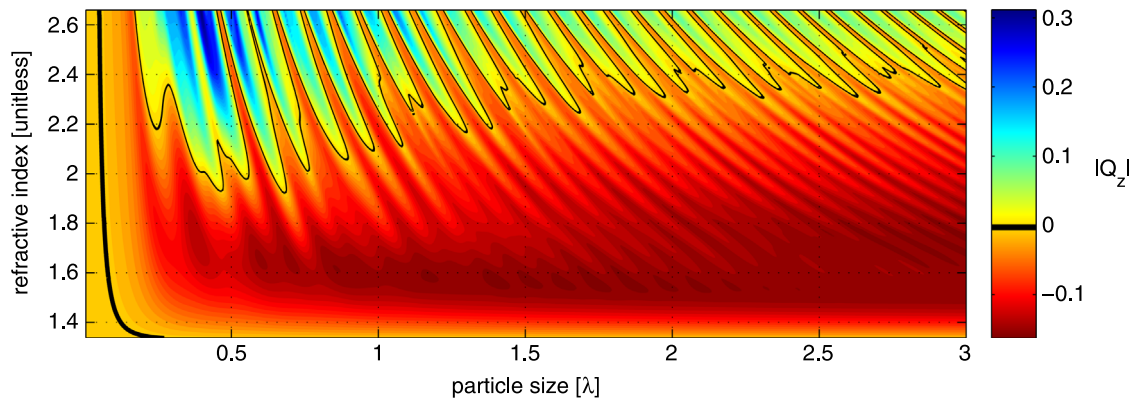


Fig. 6. Trap strength as a function of particle size and refractive index. The trapping beam is focussed by an optimally filled objective of numerical aperture 1.3, and the trapping takes place in water. The thick line represents an equipotential contour for a reasonable probability for the escape of Brownian particles. The thin line is the cutoff between particles which experience trapping and which are pushed from the focus.

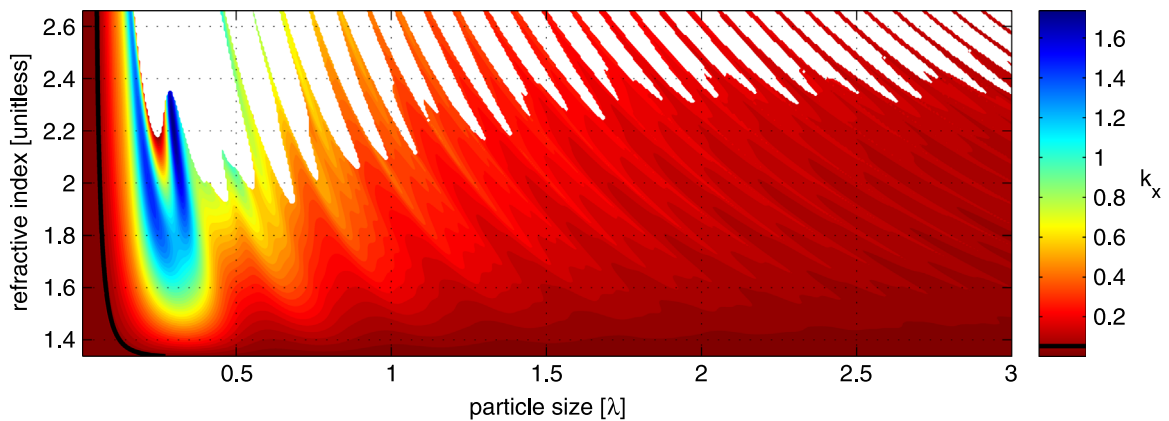


Fig. 7. Radial spring constant as a function of particle size and refractive index. The trapping beam is focussed by an optimally filled objective of numerical aperture 1.3, and the trapping takes place in water. As a trap is only viable when there is a restoring force acting upon the particle, we only show trap stiffnesses for particles which are also axially trapped. However, there is still a periodic relationship with the particle radius.

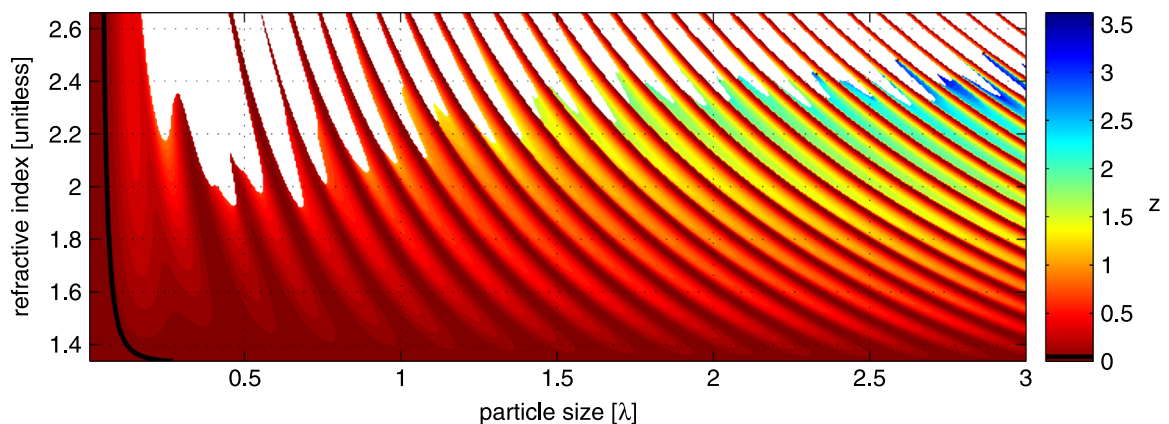


Fig. 8. Equilibrium position as a function of particle size and refractive index. The trapping beam is focussed by an optimally filled objective of numerical aperture 1.3, and the trapping takes place in water. There is no equilibrium position if the particle is not trapped (white region). As a trap is only viable when there is a restoring force acting upon the particle, we only show trap stiffnesses for particles which are also axially trapped. However, there is still a periodic relationship with the particle radius.

transfer of angular momentum. This requires the fields to carry angular momentum as well as momentum.

However, two features of the angular momentum of electromagnetic fields can be quite surprising indeed. The

first is that a beam can carry angular momentum about its axis—if angular momentum is the moment of momentum, how can the momentum and the angular momentum be parallel? The second surprise, which can partially explain

the first, is the existence of spin angular momentum. By definition, the spin density is the part of the angular momentum density that is independent of the choice of origin relative to which moments are taken [151]; it is *intrinsic angular momentum*, not dependent on our choice of coordinate system. The angular momentum density \mathbf{j} can be divided into an orbital angular momentum density \mathbf{l} and spin density \mathbf{s} . Spin is named in analogy with classical mechanics where a body can both undergo orbital motion and spin about its own axis, and the total angular momentum associated with the spinning of the body is independent of the choice of origin. However, this analogy is inexact, since in field theory it is the spin *density* which is independent of choice of origin. In general, we can write

$$\mathbf{j} = \mathbf{l} + \mathbf{s}. \quad (16)$$

The spin flux \mathbf{s} of a plane electromagnetic wave depends on its degree of circular polarisation σ , defined as

$$\sigma = (I_L - I_R)/I \quad (17)$$

where I_L and I_R are the irradiances of the left- and right-circularly polarised components [125], and is

$$\mathbf{s} = \sigma \mathbf{S}/\omega, \quad (18)$$

where \mathbf{S} is the Poynting vector and ω is the optical frequency of the time-harmonic field. This is the classical equivalent to the quantum mechanical idea that photons carry $\pm \hbar$ spin. The Cartesian components of the time-averaged spin angular momentum flux density \mathbf{s} are

$$s_i = i\epsilon_0 \epsilon_{ijk} E_j E_k^* / (2\omega), \quad (19)$$

where the expression is summed over repeated indices and the real part is taken [82,163,32]. $E_{x,y,z}$ are the Cartesian components of the complex amplitude \mathbf{E}_0 , the complex field amplitude, and ϵ_{ijk} is the Levi-Civita symbol. The orbital components are [82,163,32]

$$l_i = i\epsilon_0 E_j (\mathbf{r} \times \nabla) E_j^* / (2\omega). \quad (20)$$

These give simple results for plane waves, rays, and paraxial beams (and spherical waves in the far field, where they are locally plane). If a beam has a uniform phase over a plane, or, more generally, phase that is rotationally symmetric about the beam axis, then the orbital angular momentum flux density about the beam axis is zero. Notable exceptions to this—that is, beams which carry orbital angular momentum about the beam axis—are optical vortex beams [78,134,133,129].

It is not possible to separate the total angular momentum into spin and orbital angular momenta in a way that is both gauge independent and Lorentz invariant [83,163,32]. It is, however, possible to do so in a gauge-independent manner for time-harmonic fields. Since a non-plane wave time-harmonic field is not time-harmonic if we view it in a relatively moving frame, we can see that we have given up Lorentz-invariance of the separation.

It is common to see statements such that the angular momentum density is the moment of the linear momentum density,

$$\mathbf{j} = \mathbf{r} \times \mathbf{p} = \mathbf{nr} \times \mathbf{S}/c. \quad (21)$$

However, this cannot be correct, because it is equivalent to stating that electromagnetic waves cannot carry spin.

However, this expression *can* be used to calculate the *total* angular momentum of an electromagnetic wave, as long as the fields are finite in extent [82]. Therefore, while Eq. (21) is not the correct angular momentum density, we can still make use of it in practical calculations. The mystery of why we can use a wrong result to obtain a correct outcome can be explained if we approach the problem using Lagrangian field theory. From the Lagrangian for the electromagnetic field, the conserved quantities related to translations and rotations can be found via Noether's theorem. These are the momentum and angular momentum [83,151,84]. The canonical energy-momentum tensor (or canonical stress tensor) which this procedure gives us depends on the gauge, which motivates its transformation into the gauge-invariant symmetric energy-momentum tensor [83]. The canonical tensor gives us separate spin and orbital angular momenta, and the symmetric tensor gives us Eq. (21). The mystery is resolved when we note that the transformation from canonical tensor to symmetric tensor is only valid if the fields vanish sufficiently quickly at infinity [84]. Under exactly the same conditions, both expressions for the angular momentum density yield the same total angular momentum [82,175,138]. The situation is analogous to the existence of alternative expressions for the force density, which gives the same total force when integrated. We can approach the theoretical ambiguity here in the same spirit, and use either angular momentum density, choosing one or the other for computational convenience. That is, unless we wish to know the spin angular momentum specifically. In this case, we can calculate the spin density.

3. Computational modelling

We have considered theoretical approaches to the calculation of optical forces and torques. We will now consider the practical use of these methods. We will focus on the T-matrix method, due to its generality and efficiency. We will also consider the applicability and potential advantages of the approximate methods of Rayleigh scattering and ray optics. Finally, we will briefly discuss other approaches.

3.1. T-matrix method

The effect of a scattering object on the total electromagnetic field is often described by a *scattering matrix*. However, a diverse range of matrix descriptions of scattering has the label “scattering matrix” attached to them, and more detailed terminology is required. One of the most common scattering matrices is the *amplitude scattering matrix*, described the coherent scattering of a time-harmonic wave in a plane-wave basis. The complex amplitude of scattered field in the direction $(\theta_{\text{scat}}, \phi_{\text{scat}})$ due to an incident plane wave incident from the direction $(\theta_{\text{inc}}, \phi_{\text{inc}})$ is

$$\begin{bmatrix} E_{0\theta}^{(\text{scat})} \\ E_{0\phi}^{(\text{scat})} \end{bmatrix} = \begin{bmatrix} S_{11} & S_{12} \\ S_{21} & S_{22} \end{bmatrix} \begin{bmatrix} E_{0\theta}^{(\text{inc})} \\ E_{0\phi}^{(\text{inc})} \end{bmatrix}, \quad (22)$$

where the scattered field is given in the far field, where only the θ and ϕ components are non-zero. When considering

incoherent or partially polarised illumination, the *Müller matrix*, where the fields are described by their Stokes vectors, instead of their complex amplitudes, is useful. However, for modelling optical trapping, where our trapping beam is monochromatic, fully polarised, and coherent, it is better to use the complex amplitudes of the fields.

While the plane wave basis is, in many ways, mathematically simple, it is not most computationally convenient. One difficulty is that the set of basis functions is continuous—that is, the plane waves making up the basis can be smoothly transformed into each other. (The basis set is described by continuously varying parameters k_x and k_y (the x and y components of the wavevector) and the polarisation (transverse electric (TE) or transverse magnetic (TM))). This means that the elements of the scattering matrix, S_{ij} , are functions of the directions of incidence and scattering. A discrete basis set can lead to a more computationally friendly description of scattering.

If we begin with a discrete basis set, with basis functions $\psi_n^{(\text{inc})}$ and $\psi_n^{(\text{scat})}$, where n is a mode index labelling the functions, each ψ_n being a solution of the vector Helmholtz equation, we can write the incident field amplitude as

$$\mathbf{E}_0^{(\text{inc})} = \sum_n a_n \psi_n^{(\text{inc})}, \quad (23)$$

where a_n are the *mode amplitudes* (or *expansion coefficients*, or *beam shape coefficients*) of the incident wave. Similarly, the scattered wave can be written as

$$\mathbf{E}_0^{(\text{scat})} = \sum_k p_k \psi_k^{(\text{scat})}, \quad (24)$$

where p_k are the mode amplitudes of the scattered wave. Computationally, it will be necessary to truncate these sums at some finite n_{max} ; practical use requires a choice of basis functions where convergence of the sum occurs by this truncation. Since the resulting sets of amplitudes are finite, we can write the incident and scattered waves as column vectors \mathbf{a} and \mathbf{p} , and write their relationship in matrix form as

$$\mathbf{p} = \mathbf{T}\mathbf{a}, \quad (25)$$

where \mathbf{T} is the *T-matrix*, or transition matrix, or system transfer matrix. This description of scattering requires that the electromagnetic properties of the scattering object are linear, and constant in time. This last requirement means that the geometry of the object must be constant. In turn, this means that the scattering is described in a coordinate system fixed to the particle. (In principle, one can treat a particle with variable geometry with the T-matrix method, if the variation is slow enough to assume that we have a succession of T-matrices. We also typically assume that the incident field is monochromatic, but this is not a strict requirement; what is required is that only discrete frequencies are present (so that the basis is discrete); this would be satisfied, for example, by a periodic series of pulses.) This results in a *constant* T-matrix; the elements of the T-matrix are numbers, rather than functions of angles. The T-matrix elements are independent of the direction, polarisation, and spatial variation of the incident light.

At this point, it is useful to pause and reflect on what the T-matrix method is, and what it is not. The above

discussion essentially defines the T-matrix method; we can more concisely state this definition as a matrix description of the scattering properties of an object where the incident and scattered fields are expanded in series of suitable discrete basis functions. Even more briefly, we can write Eq. (25) as a concise expression of this definition: $\mathbf{p} = \mathbf{T}\mathbf{a}$. It has not been necessary to consider the set of basis functions in detail—we have only specified that the basis set must be discrete. For the simplest choices of coordinate system (Cartesian, cylindrical, and spherical), only the spherical coordinate system leads to a discrete basis set. Thus, for an electromagnetic scattering problem, where we want to know the electric and magnetic fields (often in order to find the scattered power and scattering pattern, but here we are more interested in using the fields to calculate the optical forces), the most common choice of basis set is the divergence-free solutions to the vector Helmholtz equation (vector spherical wavefunctions, or VSWFs; the details are given below). Indeed, some authors give definitions restricting the T-matrix method to this basis [119]. However, it seems to us to be better to retain a more general definition, allowing the use of, for example, spheroidal wavefunctions (note that [119] include such work in their database), and covering non-electromagnetic scattering, including cases where the fields are solutions of an equation other than the vector Helmholtz equation. The general definition also includes electromagnetic scattering where the electromagnetic field is given in terms of potentials rather than the electric field \mathbf{E} and the magnetic field \mathbf{H} or \mathbf{B} . This could include the vector potential \mathbf{A} and scalar potential ϕ , Hertz vectors, scalar Hertz potentials, or Bromwich potentials [55,64,54].

In the course of outlining the T-matrix method, it has not been necessary to consider how we might calculate the T-matrix or its elements, from which we can conclude that the T-matrix method is independent of whatever method we might choose to calculate the T-matrix. Thus, the T-matrix method, by itself, is not a method for calculating the scattering properties of an object, but rather a method for *describing* the scattering properties of an object. “T-matrix description of scattering” or “T-matrix formulation of scattering” are more accurately descriptive names—and are used in the literature [137,85, 87,53,127]. However, “T-matrix method” is widely used and firmly entrenched. Given the lack of a method to actually calculate the T-matrix as an integral part of the T-matrix method/formulation/description, it is necessary to choose a method; this is discussed in the following section.

Our definition of the T-matrix method includes a well-known and widely used theory of electromagnetic scattering: Lorenz–Mie theory [105,115,38,162,53] (or Mie theory, or Lorenz–Mie–Debye theory, etc.). Lorenz–Mie theory is restricted to isotropic homogeneous spheres [17], and assumes plane wave illumination. Despite these restrictions, all of the ingredients of the T-matrix method are present: the fields are written as sums of vector spherical wavefunctions, and a linear relationship is given between the incident and scattered fields (the Mie coefficients a_n and b_n [162]). Since each incident VSWF only couples to a single scattered VSWF, the T-matrix is diagonal, with the Mie coefficients being the diagonal elements. Usually, the

matrix nature of the mathematical description of scattering in Lorenz–Mie theory is left implicit, rather than stated explicitly.

The restriction to plane wave illumination in Lorenz–Mie theory can be very limiting, and the desire to model the scattering of laser beams by particles provided strong motivation for generalisation of the theory. This was achieved in the form of generalised Lorenz–Mie theory (GLMT) [55,64,54,57]. GLMT is not simply the T-matrix method restricted to spherical scatterers. The T-matrix method is a matrix description of the scattering properties of a particle, while GLMT uses such a matrix description (usually, as in Lorenz–Mie theory, implicitly), and in addition, provides a method for calculating the T-matrix (the Mie coefficients), and methods for calculating the expansion coefficients of the beam, or beam shape coefficients. While the restriction to spherical particles might appear to be quite limiting, we are very often interested in the trapping of spherical particles, or particles that can be approximated as spherical. (We can also readily treat multi-layered spheres using GLMT [132,174,81].) We will discuss the calculation of the T-matrix and the incident beam below.

A key feature of the T-matrix method that makes it very attractive for modelling optical tweezers is the efficiency of repeated calculation for different conditions of illumination by monochromatic light. This is exactly the case we encounter in optical tweezers, where the illumination varies as the particle moves within the beam, and the T-matrix description of scattering is a very attractive framework for the modelling of optical tweezers, especially when considering the need for repeated calculations. The efficiency of the method results from the separation of the descriptions of the scattering properties of the particle (written as the T-matrix) from the features of the incident illumination. Similarly, if we are using GLMT, it is useful to explicitly write it in the T-matrix formulation.

Once the T-matrix for a particle is calculated, we can then make repeated calculations of the optical force and torque for different positions and orientations within the trapping beam. We can also make calculations for different trapping beams, as long as the wavelength remains the same, allowing, for example, investigation of the optimal illumination. A simple example would be finding the minimum numerical aperture required to trap a particular particle, and a more complex example might be an evolutionary optimisation of a structured light field produced by a spatial light modulator (SLM) [69,94].

We can also note in passing that the efficiency of repeated calculations with the T-matrix method is also useful for conventional scattering problems, where one is often interested in the scattering and extinction cross-sections, averaged over all possible orientations. Such orientation averages can be found by repeated calculations for different orientations, or even analytically, since the T-matrix describes the complete scattering properties of the particle [116].

So far, we have not considered the set of basis functions in detail, having only specified that the basis set must be discrete. For the simplest choices of coordinate system (Cartesian, cylindrical, and spherical), only the spherical

coordinate system leads to a discrete basis set. The first step is to obtain a discrete basis set for solutions to the scalar Helmholtz equation (i.e., a general solution of the scalar Helmholtz equation in spherical coordinates, which can be found by the separation of variables). A general solution to the scalar Helmholtz equation $\nabla^2 A + k^2 A = 0$ is

$$A = \sum_{n=0}^{\infty} \sum_{m=-n}^n a_{nm} h_n^{(2)}(kr) Y_{nm}(\theta, \phi) + p_{nm} h_n^{(1)}(kr) Y_{nm}(\theta, \phi), \quad (26)$$

where $h_n^{(1,2)}(kr)$ are spherical Hankel functions of the first and second kinds, and $Y_{nm}(\theta, \phi)$ are spherical harmonics. The spherical harmonics can be written in terms of associated Legendre functions $P_{nm}(x)$ as

$$Y_{nm}(\theta, \phi) = c_{nm} P_{nm}(\cos \theta) \exp(m\phi), \quad (27)$$

where c_{nm} are normalisation constants. Here, we are using polar spherical coordinates, with θ being the co-latitude measured from the $+z$ -axis, and ϕ the azimuthal angle, measured from the $+x$ -axis towards the $+y$ -axis. We normalise the spherical harmonics such that

$$\int Y_{nm}(\theta, \phi) Y_{n'm'}^*(\theta, \phi) d\Omega = \delta_{nn'} \delta_{mm'}. \quad (28)$$

Because we have chosen $\exp(-i\omega t)$ for our time variation, the spherical Hankel functions of the first kind, $h_n^{(1)}(kr)$, are outgoing waves, and those of the second kind, $h_n^{(2)}(kr)$, are incoming waves. Thus, we have a division of the total field into incoming and outgoing portions. This is useful for the calculation of optical force and torque, and absorbed power. The incoming field transports momentum, angular momentum, and energy inwards through a spherical surface surrounding the origin of the coordinate system (where the particle is located), and the outgoing field transports these outwards. The differences between these incoming and outgoing fluxes give the optical force and torque, and the absorbed power.

However, the incoming field is *not* the same as the incident field; the incident field is the field that would exist if the scatterer was not present, and therefore requires both incoming and outgoing parts. Both the incoming and outgoing basis functions approach infinity as $r \rightarrow 0$, while the incident field remains finite everywhere. A useful basis set for the incident field can be constructed using the spherical Bessel functions

$$j_n(kr) = \frac{1}{2} (h_n^{(1)}(kr) + h_n^{(2)}(kr)) \quad (29)$$

instead of the incoming Hankel functions. The total field is then

$$A = \sum_{n=0}^{\infty} \sum_{m=-n}^n a_{nm} j_n(kr) Y_{nm}(\theta, \phi) + p_{nm} h_n^{(1)}(kr) Y_{nm}(\theta, \phi), \quad (30)$$

where a_{nm} describes the incident field (unlike above, where it described the *incoming* field), and p_{nm} describes the scattered field (again, unlike above, where it described the *outgoing* field).

Thus, there are two basis sets we can use: an incoming–outgoing basis, and an incident–scattered basis. The incoming–outgoing basis is ideal for performing the calculation of optical force and torque, and the incident–scattered basis is

usually used for calculations of light scattering. The T-matrix can be calculated in either basis; in our experience, the incident–scattered basis can provide a more numerically stable calculation of the T-matrix when the particle has a refractive index close to that of the surrounding medium [150]. Conversion of the T-matrix between the two bases is simple. From Eq. (29), we have $a_{nm}^{(\text{inc}/\text{scat})} = 2a_{nm}^{(\text{inc})}$ and $a_{nm}^{(\text{inc}/\text{scat})} + 2p_{nm}^{(\text{inc}/\text{scat})} = 2p_{nm}^{(\text{inc})}$, and the T-matrices in the two bases are related by $\mathbf{T}^{(\text{in}/\text{out})} = 2\mathbf{T}^{(\text{inc}/\text{scat})} + \mathbf{I}$. The T-matrix in the incoming–outgoing basis is often called the S-matrix, and written as \mathbf{S} .

We can now proceed to generate a general solution to the vector Helmholtz equation from the solution to the scalar Helmholtz equation [121,18]. For any scalar solution,

$$\mathbf{L} = \nabla\psi, \quad (31)$$

$$\mathbf{M} = -\hat{\mathbf{r}}\mathbf{L} = \nabla \times \hat{\mathbf{r}}\psi, \quad (32)$$

$$\mathbf{N} = \frac{1}{k}\nabla \times \mathbf{M}, \quad (33)$$

are solutions to the vector Helmholtz equation. Note that

$$\mathbf{M} = \frac{1}{k}\nabla \times \mathbf{N}. \quad (34)$$

\mathbf{L} is longitudinal, i.e., $\nabla \times \mathbf{L} = 0$, and \mathbf{M} and \mathbf{N} are transverse; that is, $\nabla \cdot \mathbf{M} = 0 = \nabla \cdot \mathbf{N}$. For electromagnetic scattering, we only need \mathbf{M} and \mathbf{N} , while for more general cases of scattering of vector waves, such as in elastodynamics, all three solutions are required. If we begin with our scalar solutions $h_n^{(1,2)}(kr)Y_{nm}(\theta, \phi)$, we obtain the vector spherical wavefunctions (VSWFs)

$$\mathbf{M}_{nm}^{(1,2)}(\mathbf{kr}) = N_n h_n^{(1,2)}(kr) \mathbf{C}_{nm}(\theta, \phi) \quad (35)$$

$$\begin{aligned} \mathbf{N}_{nm}^{(1,2)}(\mathbf{kr}) &= \frac{h_n^{(1,2)}(kr)}{krN_n} \mathbf{P}_{nm}(\theta, \phi) \\ &+ N_n \left(h_{n-1}^{(1,2)}(kr) - \frac{nh_n^{(1,2)}(kr)}{kr} \right) \mathbf{B}_{nm}(\theta, \phi) \end{aligned} \quad (36)$$

where $N_n = 1/\sqrt{n(n+1)}$ are normalisation constants, and $\mathbf{B}_{nm}(\theta, \phi) = r\nabla Y_n^m(\theta, \phi)$, $\mathbf{C}_{nm}(\theta, \phi) = \nabla \times (\mathbf{r}Y_n^m(\theta, \phi))$, and $\mathbf{P}_{nm}(\theta, \phi) = \hat{\mathbf{r}}Y_n^m(\theta, \phi)$ are the vector spherical harmonics. $\mathbf{M}_{nm}^{(1)}$ and $\mathbf{N}_{nm}^{(1)}$ are outward-propagating TE and TM multipole fields, while $\mathbf{M}_{nm}^{(2)}$ and $\mathbf{N}_{nm}^{(2)}$ are inward-propagating multipole fields, which we can combine to form the regular VSWFs

$$\mathbf{RgM}_{nm}(\mathbf{kr}) = \frac{1}{2} [\mathbf{M}_{nm}^{(1)}(\mathbf{kr}) + \mathbf{M}_{nm}^{(2)}(\mathbf{kr})], \quad (37)$$

$$\mathbf{RgN}_{nm}(\mathbf{kr}) = \frac{1}{2} [\mathbf{N}_{nm}^{(1)}(\mathbf{kr}) + \mathbf{N}_{nm}^{(2)}(\mathbf{kr})]. \quad (38)$$

The incident field can be written as

$$\mathbf{E}_{\text{inc}}(\mathbf{r}) = \sum_{n=1}^{\infty} \sum_{m=-n}^n a_{nm} \mathbf{RgM}_{nm}(\mathbf{kr}) + b_{nm} \mathbf{RgN}_{nm}(\mathbf{kr}) \quad (39)$$

and the scattered field as

$$\mathbf{E}_{\text{scat}}(\mathbf{r}) = \sum_{n=1}^{\infty} \sum_{m=-n}^n p_{nm} \mathbf{M}_{nm}^{(1)}(\mathbf{kr}) + q_{nm} \mathbf{N}_{nm}^{(1)}(\mathbf{kr}). \quad (40)$$

Truncating these sums at $n = n_{\text{max}}$, we can arrange the coefficients a_{nm} , b_{nm} , p_{nm} , and q_{nm} into the incident and scattered field amplitude vectors used in the T-matrix

description of scattering:

$$\mathbf{a} = (a_{1,-1}, a_{1,0}, a_{1,1}, a_{2,-2}, a_{2,-1}, \dots, a_{n_{\text{max}}, n_{\text{max}}}, b_{1,-1}, b_{1,0}, b_{1,1}, b_{2,-2}, b_{2,-1}, \dots, b_{n_{\text{max}}, n_{\text{max}}}) \quad (41)$$

$$\mathbf{p} = (p_{1,-1}, p_{1,0}, p_{1,1}, p_{2,-2}, p_{2,-1}, \dots, p_{n_{\text{max}}, n_{\text{max}}}, q_{1,-1}, q_{1,0}, q_{1,1}, q_{2,-2}, q_{2,-1}, \dots, q_{n_{\text{max}}, n_{\text{max}}}). \quad (42)$$

The radial term in each VSWF consists of spherical Bessel functions. For kr less than approximately n , $j_n(kr) \approx 0$, so that for a scatterer that is contained within a radius r_0 , convergence of the scattered field can be achieved for $n_{\text{max}} \approx kr_0$. Accurate convergence requires n_{max} somewhat above kr , and a useful formula for good convergence is $n_{\text{max}} = kr_0 + 3\sqrt[3]{kr_0}$ [19,20,18].

3.1.1. Calculation of the T-matrix

Waterman [168,169], who developed the T-matrix method, used the extended boundary condition method (EBCM), also known as the null-field method, to calculate the T-matrix. As a result, the T-matrix method and EBCM are sometimes treated as synonymous. However, the T-matrix formulation of scattering is independent of the method used for the calculation of the T-matrix [106,86,130,53,118,104,103]. A variety of methods have been used to calculate the T-matrix, and many more methods are, in principle, possible.

The EBCM is a widely used method for the calculation of the T-matrix, being used, for example, in the widely used T-matrix computer code by Mishchenko and Travis [117]. However, the EBCM is restricted to star-shaped (i.e., the radial distance of the surface from the origin can be described by a single-valued function $r(\theta, \phi)$) isotropic and homogeneous particles, and can suffer numerical difficulties for extreme geometries, such as highly elongated or highly flattened particles. Large particles also cause computational difficulty. If particles for which the EBCM is not applicable, or fails numerically, other methods must be sought. Where the EBCM is applicable and numerically reliable, it remains a fast, convenient, and accurate method of calculating the T-matrix. A key advantage of the EBCM is that it is a 2D method, requiring only surface integrals, which reduces to a 1D method for axially symmetric particles.

Often, in optical tweezers, we wish to model the trapping of spherical particles. In this case, because the VSWFs are orthogonal over a sphere, and there is no coupling between different modes for a spherical scatterer, the T-matrix is diagonal. The T-matrix elements can be obtained analytically from the Lorenz–Mie solution for scattering by a sphere [105,115,53].

For calculating the T-matrix of arbitrary particles, one of the best choices appear to be the discrete dipole approximation (DDA) [106,103]. Loke et al. [104] used the finite-difference frequency-domain method (FDFD) to calculate the T-matrix for non-uniformly anisotropic objects [104]. Nieminen et al. [127] discuss the application of the T-matrix method for the modelling of complex objects in optical traps.

3.1.2. Incident beam coefficients

In order to use the T-matrix to find the scattered field, we must begin with a known incident field—it is necessary to find with the VSWF mode amplitudes of the incident field. In principle, we can find the mode amplitudes (i.e., the TE and TM multipole coefficients) of an arbitrary field by direct calculation of the integral transform [61,51], by integrating over two concentric spherical surfaces, or one spherical surface if the field is known to be purely incoming, purely outgoing, or regular. This is the projection of the field onto the basis function, and is conceptually the same as finding the x component of a vector \mathbf{a} by the projection $a_x = \mathbf{a} \cdot \hat{\mathbf{x}}$. The integral transform can also be carried out by least-squares solution of an overdetermined linear system [131].

Since the incident field is regular, one surface is sufficient. This requires knowing the incident field over the surface. We can model the objective focussing the beam as a device that transforms the plane wavefronts of a paraxial beam incident on the back aperture of the objective to the spherical wavefronts of the non-paraxial focussed beam, subject to truncation due to the finite size of the back aperture and the finite numerical aperture.

If the incident beam is a single mode laser beam, most of the multipole coefficients will be zero. Noting that the azimuthal mode index m is the angular momentum of the mode about the z -axis, in units of \hbar per photon, the only values of m for which the mode amplitudes will be non-zero for a Gaussian beam with beam axis along the z -axis will be $m = \pm 1$, with $m = +1$ being the left-circularly polarised component, and $m = -1$ being the right-circularly polarised component [49]. The superposition of both circular polarisations will yield an elliptically or linearly polarised beam. In some cases, over values of m will have non-zero amplitudes. For example, Laguerre–Gauss beams [148,2,129], denoted $LG_{p\ell}$, carry $\ell\hbar$ orbital angular momentum per photon about the beam axis, and the total angular momentum per photon will be $(\ell \pm 1)\hbar$, leading to non-zero amplitudes for modes with $m = \ell \pm 1$.

Both direct integration and our over-determined point-matching method [131] work, but are not the most efficient possible methods [157]. They are, however, very easily used for arbitrary fields, including experimentally measured fields [4]. A very fast method is the localised approximation [59,56,51,122], which can be useful for specific types of beams (including Gaussian beams). In principle, the localised approximation can be used for arbitrary beam [50], but some initial mathematical work is required (though symbolic computation can be useful). While the computational efficiency of finding the mode amplitudes of the incident beam is not a critical factor in most cases, they need only to be calculated once for any given beam, the localised approximation can still be attractive in cases multiple incident beams are considered, such as pulsed beams treated as superpositions of monochromatic beams [113,114].

While slow in comparison to the localised approximation, calculation of the integral transform by direct integration or over-determined point-matching is usually fast enough in practice, especially for rotationally symmetric beams such as Laguerre–Gauss beams (including the $TEM_{00}=LG_{00}$ Gaussian beam).

While calculation of the incident beam expansion coefficients is necessary for use of the T-matrix method, it can also be useful for other methods of calculating the scattering of a highly non-paraxial beam. A key point is that paraxial representations of beams, including those with higher-order non-paraxial corrections [37,93], are not solutions of the Helmholtz equation or even of the Maxwell equations. Therefore, such paraxial models of beams are not suitable for use in methods where the incident field must be a solution of the Maxwell equations or the Helmholtz equation. Converting such beam to VSWF representations which are solutions of those equations can provide incident beam models that are more widely applicable [131,51,62,101].

For a tightly focussed beam, such as produced by an optimally filled or overfilled high numerical aperture objective, the beam waist w_0 is small. Good convergence of the VSWF representation of the beam is obtained if we choose the truncation parameter n_{\max} by assuming that a radius of $r = 2w_0$ enclosed the beam sufficiently well. Since we do not know the beam waist w_0 in advance, we can use the paraxial beam waist as a convenient approximation, if the beam is not too tightly focussed [131], and use a minimum truncation point of $n_{\max} = 12$ for more tightly focussed beams. It is possible to account for spherical aberration produced by the coverslip–water interface [99,100].

This gives the mode amplitudes \mathbf{a} and \mathbf{b} for a coordinate system where the beam axis coincides with the z -axis, and the focal plane is at $z=0$. We will label these origin-focussed amplitudes \mathbf{a}_0 and \mathbf{b}_0 . However, these can only be used directly in the T-matrix calculation (25) if the particle is also centred on the origin. If the particle is away from the origin of this beam-centred coordinate system, the particle-centred coordinate system in which the T-matrix is constant will be different. So that both the T-matrix and the beam are represented in the same coordinate system, it is necessary to transform one of them to the coordinate system of the other [39]. Typically, it is faster and more convenient to transform the beam, since then we only need to transform a vector, rather than a matrix (i.e., a rank-2 tensor). The transformation is linear, and known [152,36,159].

It is useful to separate the transformation into rotations and a translation. A general transformation can be carried out as a rotation, a translation along the (new) z -axis, and a second rotation. This division of the total transformation into sub-transformations is very important for computational efficiency.

Rotations can be written in terms of a matrix rotation operator as

$$\mathbf{a} = \mathbf{R}\mathbf{a}_0. \quad (43)$$

Since the radial mode index, or order, n gives the magnitude of the total angular momentum in \hbar per photon of the mode, this magnitude will remain unchanged by a rotation since the origin, about which moments are taken when finding the angular momentum, does not move. Thus, rotations will not couple modes of differing n ; the transformation matrix \mathbf{R} is sparse. A convenient recursion relation for calculating \mathbf{R} is given by Choi et al. [25].

A series of modern papers discussing rotations and their applications to GLMT is also very useful [65,167,66,67,63].

Translations involve coupling between TE and TM modes (unlike rotations) and can be written as

$$\mathbf{a} = \mathbf{A}\mathbf{a}_0 + \mathbf{B}\mathbf{b}_0, \quad (44)$$

$$\mathbf{b} = \mathbf{B}\mathbf{a}_0 + \mathbf{A}\mathbf{b}_0. \quad (45)$$

For an arbitrary translation, the transformation matrices will be full matrices, rather than sparse. This would make translations prohibitively slow to calculate. However, translations along the z -axis will not couple modes of different m ; the azimuthal mode index m is the z -component of the angular momentum and this will be unchanged by such a translation since the distance to the axis about which moments are taken is unchanged. This is the reason why we decompose a general transformation into a rotation, a translation along the z -axis, and a second rotation. Since the translation matrices \mathbf{A} and \mathbf{B} will be sparse for translations along the z -axis, we can obtain a tremendous increase in computational efficiency [170]. This gain in efficiency is exploited in other methods such as the fast multipole method (FMM) which depends heavily on such translations [40,29,16]. The translation matrices can be calculated most efficiently by using recursion relations [90,96,18,71]; our implementation of translations is taken from Videen [164], who gives a concise and simple account.

It is important to note that translations can increase the required n_{\max} for an accurate description of the beam. The n_{\max} for the original expansion of the beam, with the origin at the focus, is found by considering a surface of radius $r_0 = \min(\lambda, 2w_0)$ that sufficiently encloses the beam. If a new origin, away from the focus, is chosen the radius of this surface enclosing the beam can become greater. For a translation of distance d , a new n_{\max} can be determined using an enclosing sphere of radius $r = r_0 + d$. Since rotations do not move the origin, and do not couple the original modes to modes of differing n , n_{\max} remains unchanged by rotations.

3.1.3. Force and torque

As noted earlier, the spatial integration of the stress tensor can be carried out analytically in the framework of the T-matrix method. This is a result of the orthogonality properties of the VSWFs. Since we can disregard the volume integral in (14), the required integral is

$$\mathbf{F} = \int_S \mathbf{T} \cdot d\mathbf{A}. \quad (46)$$

We can write the stress tensor in terms of its vector components as

$$T_{ij} = \epsilon \left(E_i E_j - \frac{1}{2} \delta_{ij} |E|^2 \right) + \frac{1}{\mu} \left(B_i B_j - \frac{1}{2} \delta_{ij} |B|^2 \right) \quad (47)$$

where δ_{ij} is the Kronecker delta function. In the far-field, the radial components of the electric and magnetic fields are zero. This means that four of the nine components of the stress tensor are also zero. The only non-zero components are T_{rr} , $T_{\theta\theta}$, $T_{\phi\phi}$, $T_{\theta\phi}$, and $T_{\phi\theta}$. Since we are considering a spherical surface in the far field, the area

element is

$$d\mathbf{A} = \hat{\mathbf{r}} r^2 \sin \theta d\theta d\phi. \quad (48)$$

The integral then becomes

$$\mathbf{F} = \iint \hat{\mathbf{r}} T_{rr} r^2 \sin \theta d\theta d\phi \quad (49)$$

from which we can write the time average in terms of the complex amplitudes (instead of the instantaneous fields) as

$$\mathbf{F} = -\frac{1}{2} \iint \hat{\mathbf{r}} (\epsilon(|E_0|^2) + \mu(|H_0|^2)) r^2 \sin \theta d\theta d\phi. \quad (50)$$

In the far field, this is equivalent to integrating the Poynting vector (which is purely radial in the far field) since the field is locally a plane wave, with the electric and magnetic field amplitudes related by the impedance. This integral can be separated into the Cartesian components of the force:

$$F_z = -\frac{1}{2} \iint (\epsilon(|E_0|^2) + \mu(|H_0|^2)) r^2 \cos \theta \sin \theta d\theta d\phi, \quad (51)$$

$$F_x = -\frac{1}{2} \iint \hat{\mathbf{r}} (\epsilon(|E_0|^2) + \mu(|H_0|^2)) r^2 \sin^2 \theta \cos \phi d\theta d\phi, \quad (52)$$

and

$$F_y = -\frac{1}{2} \iint \hat{\mathbf{r}} (\epsilon(|E_0|^2) + \mu(|H_0|^2)) r^2 \sin^2 \theta \sin \phi d\theta d\phi. \quad (53)$$

The far field limits of the VSWFs are

$$\mathbf{M}_{nm} = \frac{N_n}{kr} (\mathbf{i})^{n+1} e^{-ikr} \mathbf{C}_{nm}, \quad (54)$$

$$\mathbf{N}_{nm} = \frac{N_n}{kr} (\mathbf{i})^n e^{-ikr} \mathbf{B}_{nm}. \quad (55)$$

If the fields are written as sums over the far-field limits of the VSWFs, and substituted into the integral above, the integral is a sum of products of spherical harmonics and trigonometric functions. Since the spherical harmonics are orthonormal (i.e., $\int Y_{nm} Y_{n'm'}^* d\Omega = \delta_{nn'} \delta_{mm'}$), and the product of a trigonometric function of θ or ϕ and a spherical harmonic can be expressed as a sum of spherical harmonics with mode indices equal to the original mode indices or the original mode indices ± 1 [1], this integral can be reduced to a sum of products of mode amplitudes with the same or adjacent indices n and m [42,32,128]. Similarly, the angular momentum flux can be found by integrating the moment of the momentum flux; in this case, it is important to take the moment first, and then find the far field limit. If we wish to find spin and orbital components of the torque separately, we can write the spin flux in terms of the circular polarisation, and integrate over the surface. The orbital component of the torque can be found by subtracting the spin torque from the total torque [32].

The integral of the Poynting vector gives an even simpler result for the flux of energy, so that the incident power is given by

$$P = \sum_{n=1}^{\infty} \sum_{m=-n}^n |a_{nm}|^2 + |b_{nm}|^2 \quad (56)$$

where we have chosen units for a_{nm} and b_{nm} so that no further unit conversion coefficients are needed here. This allows simple calculation of the power and the momentum flux. If we wish to calculate fields in SI units, we can divide

these mode amplitudes by $(2Zk^2)^{(1/2)}$. Stout et al. [156] discuss the issue of beam power normalisation.

We can use the power to convert the calculated force into the dimensionless force efficiency \mathbf{Q} . The axial trapping efficiency Q_z is

$$Q_z = \frac{2}{P} \sum_{n=1}^{\infty} \sum_{m=-n}^n \frac{m}{n(n+1)} \text{Re}(a_{nm}^* b_{nm} - p_{nm}^* q_{nm}) - \frac{1}{n+1} \left[\frac{n(n+2)(n-m+1)(n+m+1)}{(2n+1)(2n+3)} \right]^{1/2} \times \text{Re}(a_{nm} a_{n+1,m}^* + b_{nm} b_{n+1,m}^* - p_{nm} p_{n+1,m}^* - q_{nm} q_{n+1,m}^*). \quad (57)$$

The torque efficiency about the z-axis is

$$\tau_z = \sum_{n=1}^{\infty} \sum_{m=-n}^n m (|a_{nm}|^2 + |b_{nm}|^2 - |p_{nm}|^2 - |q_{nm}|^2) / P. \quad (58)$$

Calculation of forces and torques from the expansion coefficients of the fields has a long history in GLMT [58,64,107,57], and the expressions given in these papers are useful when using GLMT formulated in terms of Bromwich potentials. The versions given in the text above are in terms of the VSWF expansions of the fields, which are useful when using a typical T-matrix formulation.

3.1.4. A recipe for optical tweezers via the T-matrix method

We can summarise the calculation of optical forces and torques using the T-matrix method as a recipe:

1. Calculate the T-matrix.
2. Calculate the incident beam coefficients \mathbf{a}_0 and \mathbf{b}_0 in a coordinate system with the origin at the focal point of the beam.
3. (a) Transform the incident beam coefficients from the focal point centred coordinate system to a coordinate system centred on the particle.
(b) Find the scattered field coefficients, using $\mathbf{p} = \mathbf{T}\mathbf{a}$.
(c) Find the force and torque.
(d) Repeat steps in (3) for different particle positions and orientations if desired.

3.1.5. Optical Tweezers Toolbox

A free Matlab implementation of the above recipe, the *Optical Tweezers Toolbox* [128,154] is available from

- <http://www.physics.uq.edu.au/people/nieminen/software.html> (Matlab version) or
- <http://www.physics.uq.edu.au/omg/Links.html> (Matlab and C++ library).

3.1.6. Examples

As an example of the calculation of optical forces, we present results showing some of the important quantities describing optical traps (see Section 2): the trap strength, the axial equilibrium position, and the radial spring constant (Figs. 6–8). We show the variation with particle size and refractive index, for an optical trap with the trapping beam focussed by an optimally filled objective of numerical aperture 1.3. These quantities also depend on

the numerical aperture of the trapping beam, and similar “landscapes” can be generated to show this dependence.

3.2. Rayleigh approximation

We saw above that the Rayleigh approximation gives us analytical formulae for the conservative and non-conservative parts of the force (the gradient and scattering forces, respectively). However, to make use of these formulae requires calculation of the fields, and for the tightly focussed beams typically used in optical tweezers, no simple analytical formula is available for the fields; this calculation is a numerical task, and much of the attractiveness of the Rayleigh limit result evaporates.

We could consider using the T-matrix method for a very small particle. For a sufficiently small particles, we can truncate the T-matrix at $n_{\max} = 1$, retaining only the dipole terms. If we were to also discard the magnetic dipole (i.e., TE) terms, we would be left with the usual Rayleigh approximation. Since the integral giving the force in the T-matrix method is performed analytically, it is not necessary to actually calculate the fields at any point. To use the Rayleigh formulae, we would need to calculate the field and the gradient of $|E|^2$ at the location of the particle; to find the force over a region, we require the fields and gradient over the region. Therefore, in the general case, there is a very little computational gain, or even a loss, from using the Rayleigh approximation.

However, it can be possible to approximate the trapping field, with a consequent analytical result for the forces. For example, if the trapping beam is not too tightly focused, it may be possible to approximate it using the paraxial formula, or at least low-order corrections to the paraxial formula [93,37].

In addition, if it is difficult to obtain the VSWF expansion of the incident field, the Rayleigh approximation force formulae can be useful. One example might be finding the optical forces on a small particle in a waveguide, or in a time-varying field calculated by a method such as the finite-difference time-domain method (FDTD).

It is useful to examine the range of particle sizes for which the Rayleigh formulae are accurate. The forces given by the Rayleigh formulae and the dipole-only T-matrix method, and the exact force are compared in Fig. 9, showing that the Rayleigh formulae are accurate for particles less than 1/10 of a wavelength in radius, as expected [74].

The Rayleigh approximation provides simple and clear results for the scaling of gradient, scattering, and absorption forces for small particles, and, if a suitable approximation for the trapping field can be made, can allow analytical formulae for these forces. This possibility of analytical results, even if only approximate due to simplification of the beam, is perhaps the most useful contribution to the computation of forces from the Rayleigh approximation, as well as being useful for understanding the physical processes acting in optical tweezers.

3.3. Ray optics

While the theoretical benefit of the Rayleigh approximation is clear, with the identification of gradient and

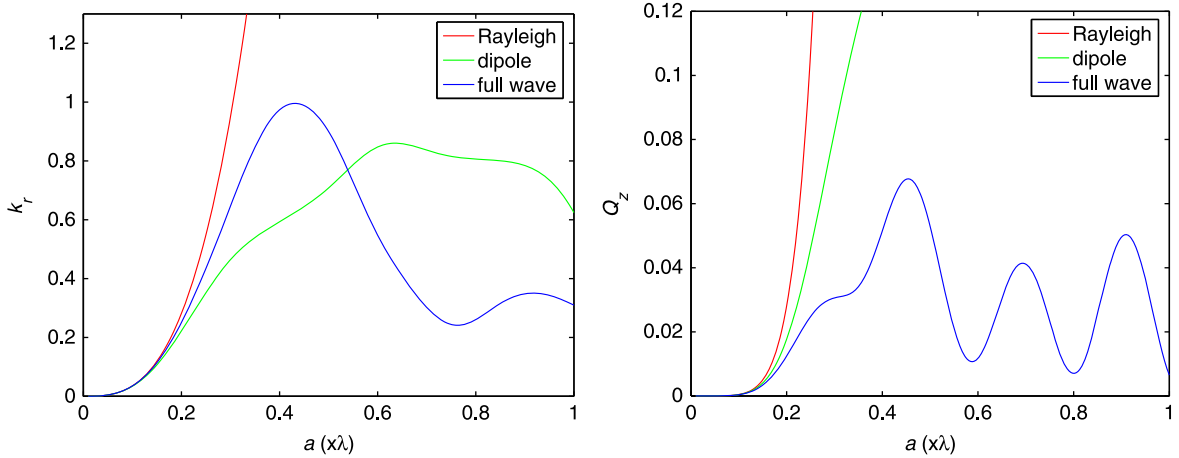


Fig. 9. Comparison between Rayleigh scattering forces and exact results. For a particle at the focus, the gradient force is zero, and the total force is the scattering force (left). The gradient force is purely responsible for the radial spring constant (right). The comparison shows the force given by the Rayleigh approximation force formulae, the T-matrix method with the T-matrix truncated at $n_{\max} = 1$, and the exact result. The Rayleigh formulae are accurate for particles less than $1/10$ of a wavelength in radius.

scattering forces, the situation is less clear with the geometric optics approximation. We can distinguish between two distinct forces when a ray interacts with a surface—reflection forces, and refraction forces. This invites an identification between reflection forces and the scattering force, and refraction forces and the gradient force [9]. However, for any given ray, it is possible for the ray to undergo both refraction and reflection as it passes through the trapped particle, preventing a clear separation of these forces. However, it is reasonable to label the force due to any ray that has been reflected, whether or not it has also undergone refraction, as a reflection force, especially since the reflection coefficient is relatively small due to the small refractive index contrast between the trapped particle and the surrounding medium (if the reflectivity is not small, the particle is typically not trapped, as the reflection forces push it out of the trap).

The geometric optics approximation is often described as a large particle approximation. That the particle be large is indeed a requirement, but we also require radii of curvature of the surface of the particle to be large compared to the wavelength, and so on. We will note an important additional requirement later, but for the moment, we can see that these conditions will be satisfied by a spherical particle that is large compared to the wavelength. For the scattering force acting on a particle at the focus of the trapping beam, the rays all meet the particle surface at normal incidence. If we make the approximation of only including single reflections from the first and second surfaces, the scattering force will be

$$\mathbf{F}_{\text{scat}} = 4R\mathbf{p} = 4\left(\frac{m-1}{m+1}\right)^2 \mathbf{p}, \quad (59)$$

where \mathbf{p} is the momentum flux of the beam (which will be less than nP/c which we would have for a parallel beam of power P , due to the convergence of the beam), and R is the Fresnel reflection coefficient at normal incidence. (For simplicity, this assumes that the power incident on the first and second surfaces is the same; this over-estimates

the reflection force by 3%.) The momentum flux can be calculated numerically. This ray optics scattering force is compared with the exact result in Fig. 10. It is immediately obvious that the ray optics scattering force is a poor approximation, for spherical particles of any size.

The radial spring constant can also be simply calculated. Each surface will cause the centre of the beam to deviate away from the original beam axis, by an amount depending on the radial displacement of the particle from the axis and the optical power of the curved surface. Neglecting spherical aberration, the power of each surface of the sphere is given by $P_{\text{opt}} = (n_{\text{particle}} - n_{\text{medium}})$, and the radial spring constant will be

$$k_r = \frac{F_r}{x} = 2\frac{P_{\text{opt}}}{n_{\text{medium}}}|p| = 2\frac{m-1}{a}|p|, \quad (60)$$

where x is the radial displacement of the sphere from the beam axis, and a is the radius of the sphere. (For simplicity, the reduction in power due to reflection is neglected. This will result in an overestimate of the spring constant of approximately 3%.) The ray optics and exact radial spring constants are compared in Fig. 10. Considering the difference between the ray optics and the exact scattering forces, the agreement for the spring constant is surprisingly good. The ray optics spring constant is systematically above the exact curve due to the neglect of reflection; if this was included, the exact curve would vary about the ray optics curve.

In both cases, the exact result shows rapid variation of the force with particle size. This is due to interference effects, which are ignored in the ray optics calculation. Essentially, if light reflected from the front surface of the sphere interferes constructively with light reflected from the rear surface, the reflectivity is increased. If the interference is destructive, the reflectivity is decreased. This strongly affects the scattering force from large spheres [108,155], and consequently affects the equilibrium position of trapped particles along the beam axis. Since the geometric optics approximation neglects such interference

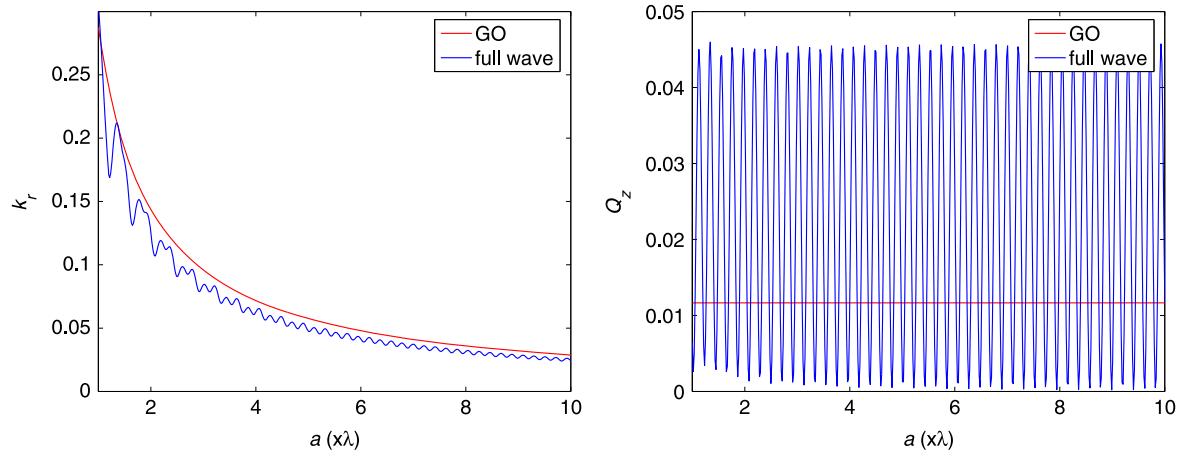


Fig. 10. Comparison between ray optics forces and exact results. For a particle at the focus, the gradient force is zero, and the total force is the scattering force (left). The gradient force is purely responsible for the radial spring constant (right). The ray optics result is very poor for the scattering force, and surprisingly accurate for the radial spring constant. The ray optics spring constant is systematically above the exact curve due to the neglect of reflection; if this was included, the exact curve would vary about the ray optics curve.

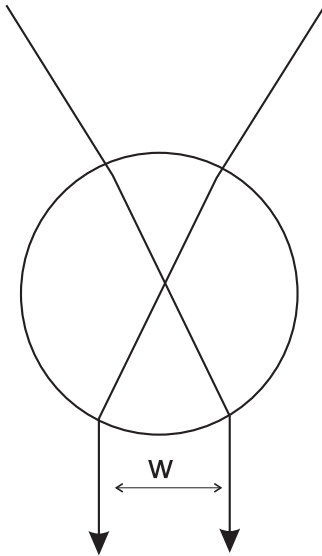


Fig. 11. Ray optics prediction of axial trap strength. The maximum axial restoring force against the direction of propagation occurs when the transmitted beam emerges as parallel as possible. If the beam width w of the emergent beam is not sufficiently large compared to the wavelength, the beam will be divergent, rather than parallel, even if the indicative rays emerge parallel.

effects, the geometric optics calculation completely fails to predict this effect, even for large spheres where the approximation is usually assumed to be accurate. Since the refractive index difference between the particle and the surrounding medium is small (or the particle would be too reflective to be able to be trapped), only a small fraction of the light will be reflected, whether the reflectivity is high or low. From the conservation of energy, it is clear that the absolute variation in the reflected power must be the same as the variation in the transmitted power. However, this variation is a large relative variation in the reflected power, and only a small relative variation

in the transmitted power. Thus, the ripples in the scattering force are large, and the ripples in the gradient force are small.

This is the first additional condition we find for ray optics to be accurate: interference effects must be negligible. The failure to predict the strong variation of scattering force with size due to interference is not entirely a bad thing. The effect seen in Fig. 10 is for a perfect sphere, and this is an idealisation that is often not matched by the actual particle within the trap. For a less perfectly spherical large particle, the optical path length for different rays can easily vary by a wavelength, which would result in an averaging of such interference effects in practice. Thus, the ray optics result can more accurately model the real particle, by automatically including this averaging [112].

The small change in the transmitted power with particle size means that we can consider interference effects small enough to ignore even if they strongly affect the scattering force. As a result, the ray optics gradient force is a good prediction of the exact gradient force. Interestingly, this is true even for spheres well below the sizes often considered to be necessary for accuracy of the geometric optics approximation (typically $a \approx 5\lambda$ or greater).

From this, we can see that the geometric optics approximation can give quantitatively accurate results for some elements of optical trapping, but gives poor results for others. One important parameter of optical traps that is poorly predicted is the axial trap strength—even when other results, such as the spring constant and radial trap strength, are given accurately, the axial trap strength (i.e., the maximum restoring force in the direction opposite to the beam propagation direction, which is an important parameter since this is usually the weakest direction of trapping) can be incorrectly given by a factor of 2 by geometric optics [88,126].

This is a special case of a more general failure of geometric optics—the focal region of the beam is not accurately represented. As the most obvious example of this, ray optics predicts a focal spot of zero width and

infinite irradiance, which we do not obtain in reality. This is the second addition condition for applicability of the ray optics approximation. Surfaces which interact with the rays must lie where the focused beam is accurately modeled by rays. That is, all such surfaces must lie in the far-field of the beam, away from the focus, where the wavefronts are spherical and the angular variation of intensity does not change with propagation. This is an important difference between ray optics modeling of the interaction of an object with a focused beam and with a plane wave—in the latter case, this condition is automatically satisfied everywhere. With a focused beam, we must make sure that no surface is near the focus. Unfortunately, the maximum axial restoring force often occurs when the near surface is near the focus, and the axial trap strength is poorly predicted (Fig. 11).

With the ray optics approximation, we see that good quantitative results can be obtained even for particles smaller than the usually accepted regime of applicability of the approximation. On the other hand, we find an additional condition of applicability, that all surfaces of the particle must be away from the focus.

However, we also find that exact methods of calculating the optical forces grow linearly with particle size, or worse (sometimes much worse!), while the computational demands of ray optics are independent of particle size. Therefore, ray optics remains a potentially valuable computational tool, making some calculations of interest feasible, or feasible in the absence of a supercomputer, even if some caution is required.

In addition, ray optics provides an averaging over interference effects due to particle size that can either cause the model to fail or can be highly beneficial, depending on the situation. For example, if we are considering a large particle that is only approximately spherical, such as a large animal cell, we would not expect to see strong interference effects, since the departure from exact sphericity will lead to averaging of such effects. Since the ray optics model provides this averaging with no further computational overhead, it can be the ideal method for calculating optical forces, as long as the surface of the particle is away from the focus.

3.4. Other approaches to computational modelling

A variety of other methods can be used for modelling optical tweezers. Where particles are too large for the Rayleigh approximation, too small for ray optics (or interference effects are important), and have geometries that prevent the use of Lorenz–Mie theory or simple T-matrix calculation methods such as EBCM, other methods must be used. Many of these alternative methods could be used to either calculate the T-matrix [127] or to directly calculate the optical forces. Which of these is the better option depends on to what extent repeated calculations are required. A broadly usable method for calculating the T-matrix by such general methods is to calculate it column-by-column, by solving the scattering problem for illumination consisting of single-mode VSWF fields [130]. This requires approximately $4n_{\max}$ separate scattering calculations. If this is significantly smaller than the

repeated calculations required, it is better to calculate the T-matrix, and then use that to find the optical forces and torques. This also has the advantage of analytical integration to find the force from the momentum flux.

Some candidate methods are the finite element method [172,171], the finite-difference time-domain (FDTD) method [47,141], and the discrete-dipole approximation (DDA) [80,149]. DDA provides an interesting example, since the particle is represented as a collection of dipoles, and the Rayleigh force formulae can be used to determine the force on each dipole. In this way, internal stresses within the particle can be found.

4. Conclusion

We have reviewed the theory and computational modelling of optical tweezers. Our discussion of computational modelling focussed on the T-matrix method, which is an attractive method for calculating the optical forces for two main reasons: it is very efficient for repeated calculations, and allows accurate calculation of the force via analytical integration of the stress tensor (expressed as a sum of products of field expansion coefficients). A free Matlab implementation is available [128,154].

Approximate methods such as Rayleigh scattering provide theoretical insight that is lacking in purely numerical methods. In addition, such approximate methods remain useful in their regimes of applicability.

A great deal of work remains in modelling optical trapping. Possible topics for further work include improved methods for the modelling of arbitrary particles, including complex media such as anisotropic particles and particles composed of metamaterials, the modelling of non-optical forces, including contact between particles, and particles and their surroundings, modelling of fluid flow, including hydrodynamic interaction between particles and the modelling of convective flow. Other problems include particles with non-linear electromagnetic properties, particles that are deformable or otherwise change shape, trapping in media with complex optical properties, and problems with a large range of important length scales. Thus, it can be seen that, although a great deal of productive work has been done, much remains, and the interested researcher can usefully invest much time at the coal-face of modelling optical tweezers.

References

- [1] Abramowitz M, Stegun IA., editors. Handbook of mathematical functions with formulas, graphs, and mathematical tables. Washington, DC: National Bureau of Standards; 1964.
- [2] Allen L, Beijersbergen MW, Spreeuw RJC, Woerdman JP. Orbital angular momentum and the transformation of Laguerre–Gaussian laser modes. *Phys Rev A* 1992;45:8185–9.
- [3] Allison SA. A Brownian dynamics algorithm for arbitrary rigid bodies. Application to polarized dynamic light scattering. *Macromolecules* 1991;24(2):530–6.
- [4] Asavei T, Loke VLY, Barbieri M, Nieminen TA, Heckenberg NR, Rubinsztein-Dunlop H. Optical angular momentum transfer to microrotors fabricated by two-photon photopolymerization. *New J Phys* 2009;11:093021.
- [5] Asavei T, Nieminen TA, Loke VLY, Stilgoe AB, Bowman R, Padgett MJ, et al. Optically trapped and driven paddle-wheel. *New J Phys* 2013;15:063016.

- [6] Ashkin A. Acceleration and trapping of particles by radiation pressure. *Phys Rev Lett* 1970;24:156–9.
- [7] Ashkin A. Optical trapping and manipulation of neutral particles using lasers. *Proc Natl Acad Sci USA* 1997;94:4853–60.
- [8] Ashkin A. Optical trapping and manipulation of neutral particles using lasers. Singapore: World Scientific; 2007.
- [9] Ashkin A, Dziedzic JM, Bjorkholm JE, Chu S. Observation of a single-beam gradient force optical trap for dielectric particles. *Opt Lett* 1986;11:288–90.
- [10] Bartoli A. Il calorico raggianti e il secondo principio di termodinamica. *Il Nuovo Cimento* 1884;15:193–202.
- [11] Barton JP, Alexander DR, Schaub SA. Internal and near-surface electromagnetic fields for a spherical particle irradiated by a focused laser beam. *J Appl Phys* 1988;64:1632–9.
- [12] Barton JP, Alexander DR, Schaub SA. Theoretical determination of net radiation force and torque for a spherical particle illuminated by a focused laser beam. *J Appl Phys* 1989;66:4594–602.
- [13] Berns MW. Optical tweezers: tethers, wavelengths, and heat. *Methods Cell Biol* 2007;82:455, 457–466.
- [14] Beyer RT. Radiation pressure—the history of a mislabeled tensor. *J Acoust Soc Am* 1978;63(4):1025–30.
- [15] Bishop AI, Nieminen TA, Heckenberg NR, Rubinsztein-Dunlop H. Optical application and measurement of torque on microparticles of isotropic nonabsorbing material. *Phys Rev A* 2003;68:033802.
- [16] Board J, Schulten K. The fast multipole algorithm. *Comput Sci Eng* 2000;2(1):76–9.
- [17] Bohren CF. Scattering by particles. In: Bass M, Van Stryland EW, Williams DR, Wolfe WL, editors. *Handbook of optics*, vol. 1. 2nd ed. New York: McGraw-Hill, 1995, p. 6.1–21 [Chapter 6].
- [18] Brock BC. Using vector spherical harmonics to compute antenna mutual impedance from measured or computed fields. Sandia Report SAND2000-2217-Revised. Albuquerque, New Mexico, USA: Sandia National Laboratories; 2001.
- [19] Bruning JH, Lo YT. Multiple scattering of EM waves by spheres. Part I—multipole expansion and ray-optical solutions. *IEEE Trans Antennas Propag* 1971;19(3):378–90.
- [20] Bruning JH, Lo YT. Multiple scattering of EM waves by spheres. Part II—numerical and experimental results. *IEEE Trans Antennas Propag* 1971;19(3):391–400.
- [21] Bui AAM, Stilgoe AB, Nieminen TA, Rubinsztein-Dunlop H. Calibration of nonspherical particles in optical tweezers using only position measurement. *Opt Lett* 2013;38(8):1244–6.
- [22] Cao Y, Stilgoe AB, Chen L, Nieminen TA, Rubinsztein-Dunlop H. Equilibrium orientations and positions of non-spherical particles in optical traps. *Opt Express* 2013;20(12):12987–96.
- [23] Chaumet PC, Nieto-Vesperinas M. Coupled dipole method determination of the electromagnetic force on a particle over a flat dielectric surface. *Phys Rev B* 2000;61:14119–27.
- [24] Chaumet PC, Nieto-Vesperinas M. Time-averaged total force on a dipolar sphere in an electromagnetic field. *Opt Lett* 2000;25:1065–7.
- [25] Choi CH, Ivanic J, Gordon MS, Ruedenberg K. Rapid and stable determination of rotation matrices between spherical harmonics by direct recursion. *J Chem Phys* 1999;111:8825–31.
- [26] Chu LJ, Haus HA, Penfield Jr. P. The force density in polarizable and magnetizable fluids. *Proc IEEE* 1966;54(7):920–35.
- [27] Chu S. The manipulation of neutral particles. *Rev Mod Phys* 1998;70:685–706.
- [28] Cohen-Tannoudji CN. Manipulating atoms with photons. *Rev Mod Phys* 1998;70:707–19.
- [29] Coifman R, Rokhlin V, Wandzura S. The fast multipole method for the wave equation: a pedestrian prescription. *IEEE Antennas Propag Mag* 1993;35:7–12.
- [30] Constantinou VN. *Laminar viscous flow*. New York: Springer; 1995.
- [31] Cornell EA, Wieman CE. Bose–Einstein condensation in a dilute gas, the first 70 years and some recent experiments. *Rev Mod Phys* 2002;74:875–93.
- [32] Crichton JH, Marston PL. The measurable distinction between the spin and orbital angular momenta of electromagnetic radiation. *Electron J Differ Equ Conf* 2000;4:37–50.
- [33] Crookes W. On attraction and repulsion accompanying radiation. *Proc Phys Soc Lond* 1874;1:35–51.
- [34] Crookes W. On attraction and repulsion resulting from radiation. *Philos Trans R Soc Lond* 1874;164:501–27.
- [35] Crookes W. On repulsion resulting from radiation—Part II. *Philos Trans R Soc Lond* 1875;165:519–47.
- [36] Cruzan OR. Translational addition theorems for spherical vector wave functions. *Q Appl Math* 1962;20(1):33–40.
- [37] Davis LW. Theory of electromagnetic beams. *Phys Rev A* 1979;19:1177–9.
- [38] Debye P. Der Lichtdruck auf Kugeln von beliebigem Material. *Ann Phys* 1909;30:57–136.
- [39] Doicu A, Wriedt T. Computation of the beam-shape coefficients in the generalized Lorenz–Mie theory by using the translational addition theorem for spherical vector wave functions. *Appl Opt* 1997;36:2971–8.
- [40] Engheta N, Murphy WD, Rokhlin V, Vassiliou MS. The fast multipole method (FMM) for electromagnetic scattering problems. *IEEE Trans Antennas Propag* 1992;40(6):634–41.
- [41] Euler L. Memoire sur l'effet de la propagation successive de la lumiere dans l'apparition tant des planetes que des cometes. *Mem Acad Sci Berl* 1746;2:141–81.
- [42] Farsund Ø, Felderhof BU. Force, torque, and absorbed energy for a body of arbitrary shape and constitution in an electromagnetic radiation field. *Physica A* 1996;227:108–30.
- [43] Fernandes MX, Garcia de la Torre J. Brownian dynamics simulation of rigid particles of arbitrary shape in external fields. *Biophys J* 2002;83(6):3039–48.
- [44] Frankel E. Corpuscular optics and the wave theory of light: the science and politics of a revolution in physics. *Soc Stud Sci* 1976;6(2):141–84.
- [45] Gahagan KT, Swartzlander GA. Optical vortex trapping of particles. *Opt Lett* 1996;21:827–9.
- [46] García de la Torre JG, Bloomfield VA. Hydrodynamic properties of complex, rigid, biological macromolecules: theory and applications. *Q Rev Biophys* 1981;14(1):81–139.
- [47] Gauthier RC. Computation of the optical trapping force using an FDTD based technique. *Opt Express* 2005;13(10):3707–18.
- [48] Gordon JP. Radiation forces and momenta in dielectric media. *Phys Rev A* 1973;8:14–21.
- [49] Gouesbet G. Partial-wave expansions and properties of axisymmetric light beams. *Appl Opt* 1996;35:1543–55.
- [50] Gouesbet G. Validity of the localized approximation for arbitrary shaped beams in the generalized Lorenz–Mie theory for spheres. *J Opt Soc Am A* 1999;16:1641–50.
- [51] Gouesbet G. Generalized Lorenz–Mie theories, the third decade: a perspective. *J Quant Spectrosc Radiat Transf* 2009;110:1223–38.
- [52] Gouesbet G. On the optical theorem and non-plane-wave scattering in quantum mechanics. *J Math Phys* 2009;50(11):112302.
- [53] Gouesbet G. T-matrix formulation and generalized Lorenz–Mie theories in spherical coordinates. *Opt Commun* 2010;283:517–21.
- [54] Gouesbet G. A scientific story of generalized Lorenz–Mie theories with epistemological remarks. *J Quant Spectrosc Radiat Transf* 2013;126:7–15.
- [55] Gouesbet G, Gréhan G. Sur la généralisation de la théorie de Lorenz–Mie. *J Opt (Paris)* 1982;13(2):97–103 [On the scattering of light by a Mie scatterer located on the axis of an axisymmetric light profile].
- [56] Gouesbet G, Gréhan G. Generic formulation of a generalized Lorenz–Mie theory for a particle illuminated by laser pulses. *Part Part Syst Charact* 2000;17:213–24.
- [57] Gouesbet G, Gréhan G. *Generalized Lorenz–Mie theories*. Berlin: Springer; 2011.
- [58] Gouesbet G, Gréhan G, Maheu B. Scattering of a Gaussian beam by a Mie scatterer center using a Bromwich formalism. *J Opt (Paris)* 1985;16(2):83–9.
- [59] Gouesbet G, Gréhan G, Maheu B. Expressions to compute the coefficients g_n^m in the generalized Lorenz–Mie theory using finite series. *J Opt (Paris)* 1988;19(1):35–48.
- [60] Gouesbet G, Letellier C, Gréhan G, Hodges JT. Generalized optical theorem for on-axis Gaussian beams. *Opt Commun* 1996;125(1):137–57.
- [61] Gouesbet G, Letellier C, Ren KF, Gréhan G. Discussion of two quadrature methods of evaluating beam-shape coefficients in generalized Lorenz–Mie theory. *Appl Opt* 1996;35:1537–42.
- [62] Gouesbet G, Lock JA. List of problems for future research in generalized Lorenz–Mie theories and related topics, review and prospectus. *Appl Opt* 2013;52:897–916.
- [63] Gouesbet G, Lock JA, Wang JJ, Gréhan G. Transformations of spherical beam shape coefficients in generalized Lorenz–Mie theories through rotations of coordinate systems. V. Localized beam models. *Opt Commun* 2011;284:411–7.
- [64] Gouesbet G, Maheu B, Gréhan G. Light scattering from a sphere arbitrarily located in a Gaussian beam, using a Bromwich formulation. *J Opt Soc Am A* 1988;5(9):1427–43.
- [65] Gouesbet G, Wang JJ, Han YP. Transformations of spherical beam shape coefficients in generalized Lorenz–Mie theories through rotations of coordinate systems: I. General formulation. *Opt Commun* 2010;283:3218–25.

- [66] Gouesbet G, Wang JJ, Han YP. Transformations of spherical beam shape coefficients in generalized Lorenz–Mie theories through rotations of coordinate systems: III. Special values of Euler angles. *Opt Commun* 2010;283:3235–43.
- [67] Gouesbet G, Wang JJ, Han YP, Grehan G. Transformations of spherical beam shape coefficients in generalized Lorenz–Mie theories through rotations of coordinate systems IV. Plane waves. *Opt Commun* 2010;283:3244–54.
- [68] Grehan G, Gouesbet G. Optical levitation of a single particle to study the theory of the quasi-elastic scattering of light. *Appl Opt* 1980;19:2485–7.
- [69] Grier DG. A revolution in optical manipulation. *Nature* 2003;424 (August):810–6.
- [70] Guilloteau F, Bréhan G, Gouesbet G. Optical levitation experiments to assess the validity of the generalized Lorenz–Mie theory. *Appl Opt* 1992;31(May (15)):2942–51.
- [71] Gumerov NA, Duraiswami R. Recursions for the computation of multipole translation and rotation coefficients for the 3-D Helmholtz equation. *SIAM J Sci Comput* 2003;25(4):1344–81.
- [72] Gussgard R, Lindmo T, Brevik I. Calculation of the trapping force in a strongly focused laser beam. *J Opt Soc Am B* 1992;9(October (10)):1922–30.
- [73] Hansen PM, Bhatia VK, Harrit N, Oddershede L. Expanding the optical trapping range of gold nanoparticles. *Nano Lett* 2005;5(10):1937–42.
- [74] Harada Y, Asakura T. Radiation forces on a dielectric sphere in the Rayleigh scattering regime. *Opt Commun* 1996;124:529–41.
- [75] Hardin CL. The scientific work of the Reverend John Michell. *Ann Sci* 1966;22:27–47.
- [76] Hawes C, Osterrieder A, Sparkes IA, Ketelaar T. Optical tweezers for the micromanipulation of plant cytoplasm and organelles. *Curr Opin Plant Biol* 2010;13(6):731–5.
- [77] Heaviside O. On the forces, stresses, and fluxes of energy in the electromagnetic field. *Philos Trans R Soc Lond A* 1892;183:423–80.
- [78] Heckenberg NR, McDuff R, Smith CP, Rubinsztein-Dunlop H, Wegener MJ. Laser beams with phase singularities. *Opt Quantum Electron* 1992;24:S951–62.
- [79] Heidarzadeh T. A history of physical theories of comets, from Aristotle to Whipple. Springer; Dordrecht; 2008.
- [80] Hoekstra AG, Frijlink M, Waters LBFM, Sloot PMA. Radiation forces in the discrete-dipole approximation. *J Opt Soc Am A* 2001;18:1944–53.
- [81] Hu Y, Nieminen TA, Heckenberg NR, Rubinsztein-Dunlop H. Anti-reflection coating for improved optical trapping. *J Appl Phys* 2008;103:093119.
- [82] Humblet J. Sur le moment d'impulsion d'une onde électromagnétique. *Physica* 1943;10(7):585–603.
- [83] Jackson JD. Classical electrodynamics. 3rd ed. New York: John Wiley; 1999.
- [84] Jauch JM, Rohrlich F. The theory of photons and electrons. 2nd ed. New York: Springer; 1976.
- [85] Kahnert FM. Numerical methods in electromagnetic scattering theory. *J Quant Spectrosc Radiat Transf* 2003;79–80:775–824.
- [86] Kahnert FM, Stamnes JJ, Stamnes K. Surface-integral formulation for electromagnetic scattering in spheroidal coordinates. *J Quant Spectrosc Radiat Transf* 2003;77:61–78.
- [87] Kahnert M. Irreducible representations of finite groups in the T-matrix formulation of the electromagnetic scattering problem. *J Opt Soc Am A* 2005;22(6):1187–99.
- [88] Kawauchi H, Yonezawa K, Kozawa Y, Sato S. Calculation of optical trapping forces on a dielectric sphere in the ray optics regime produced by a radially polarized laser beam. *Opt Lett* 2007;32(13):1839–41.
- [89] Ketterle W. When atoms behave as waves: Bose–Einstein condensation and the atom laser. *Rev Mod Phys* 2002;74:1131–51.
- [90] Kim KT. The translation formula for vector multipole fields and the recurrence relations of the translation coefficients of scalar and vector multipole fields. *IEEE Trans Antennas Propag* 1996;44(11):1482–7.
- [91] Knoner G, Parkin S, Nieminen TA, Heckenberg NR, Rubinsztein-Dunlop H. Measurement of the index of refraction of single microparticles. *Phys Rev Lett* 2006;97:157402.
- [92] Lang MJ, Block SM. Resource Letter: LBOT-1: laser-based optical tweezers. *Am J Phys* 2003;71(3):201–15.
- [93] Lax M, Louisell WH, McKnight WB. From Maxwell to paraxial wave optics. *Phys Rev A* 1975;11:1365–70.
- [94] Leach J, Wulff K, Sinclair G, Jordan P, Courtial J, Thomson L, et al. Interactive approach to optical tweezers control. *Appl Opt* 2006;45(5):897–903.
- [95] Ledebew P. An experimental investigation of the pressure of light. *Astrophys J* 1902;15:60–2.
- [96] Xu Y-l. Efficient evaluation of vector translation coefficients in multiparticle light-scattering theories. *J Comput Phys* 1998;139:137–65.
- [97] Liouville J. Note sur la theorie de la variation des constantes arbitraires. *J Math* 1838;3:342–9.
- [98] Lock JA. Failure of the optical theorem for Gaussian-beam scattering by a spherical particle. *J Opt Soc Am A* 1995;12:2708–15.
- [99] Lock JA. Calculation of the radiation trapping force for laser tweezers by use of generalized Lorenz–Mie theory. I. Localized model description of an on-axis tightly focused laser beam with spherical aberration. *Appl Opt* 2004;43(12):2532–44.
- [100] Lock JA. Calculation of the radiation trapping force for laser tweezers by use of generalized Lorenz–Mie theory. II. On-axis trapping force. *Appl Opt* 2004;43(12):2545–54.
- [101] Lock JA. Beam shape coefficients of the most general focused Gaussian laser beam for light scattering applications. *J Quant Spectrosc Radiat Transf* 2013;126:16–24.
- [102] Loke VLY, Asavei T, Nieminen TA, Heckenberg NR, Rubinsztein-Dunlop H. Optimization of optically-driven micromachines. *Proc SPIE* 2009;7400:74001Z.
- [103] Loke VLY, Nieminen TA, Heckenberg NR, Rubinsztein-Dunlop H. T-matrix calculation via discrete dipole approximation, point matching and exploiting symmetry. *J Quant Spectrosc Radiat Transf* 2009;110:1460–71.
- [104] Loke VLY, Nieminen TA, Parkin SJ, Heckenberg NR, Rubinsztein-Dunlop H. FDFD/T-matrix hybrid method. *J Quant Spectrosc Radiat Transf* 2007;106:274–84.
- [105] Lorenz L. Lysbevægelsen i og uden for en af plane Lysbølger belyst Kugle. *Vidensk Selsk Skr* 1890;6:2–62.
- [106] Mackowski DW. Discrete dipole moment method for calculation of the T matrix for nonspherical particles. *J Opt Soc Am A* 2002;19(5):881–93.
- [107] Maheu B, Gouesbet G, Grehan G. A concise presentation of the generalized Lorenz–Mie theory for arbitrary location of the scatterer in an arbitrary incident profile. *J Opt (Paris)* 1988;19(2):59–67.
- [108] Maia Neto PA, Nussenzweig HM. Theory of optical tweezers. *Europhys Lett* 2000;50:702–8.
- [109] Martinot-Lagarde G, Pouligny B, Angelova MI, Gréhan G, Gouesbet G. Trapping and levitation of a dielectric sphere with off-centred Gaussian beams: II GLMT analysis. *Pure Appl Opt* 1995;4:571–85.
- [110] Maxwell JC. A dynamical theory of the electromagnetic field. *Philos Trans R Soc Lond* 1865;155:459–512.
- [111] Maxwell JC. A treatise on electricity and magnetism. Oxford: Clarendon Press; 1873 in two volumes.
- [112] Mazolli A, Maia Neto PA, Nussenzweig HM. Theory of trapping forces in optical tweezers. *Proc R Soc Lond A* 2003;459:3021–41.
- [113] Mees L, Gouesbet G, Gréhan G. Scattering of laser pulses (plane wave and focused Gaussian beam) by spheres. *Appl Opt* 2001;40:2546–50.
- [114] Mees L, Gréhan G, Gouesbet G. Time-resolved scattering diagrams for a sphere illuminated by plane wave and focused short pulses. *Opt Commun* 2001;194(1):59–65.
- [115] Mie G. Beiträge zur Optik trüber Medien, speziell kolloidaler Metallosungen. *Ann Phys* 1908;25(3):377–445.
- [116] Mishchenko MI. Light scattering by randomly oriented axially symmetric particles. *J Opt Soc Am A* 1991;8:871–82.
- [117] Mishchenko MI, Travis LD. Capabilities and limitations of a current FORTRAN implementation of the T-matrix method for randomly oriented, rotationally symmetric scatterers. *J Quant Spectrosc Radiat Transf* 1998;60:309–24.
- [118] Mishchenko MI, Travis LD, Mackowski DW. T-matrix method and its applications to electromagnetic scattering by particles: a current perspective. *J Quant Spectrosc Radiat Transf* 2010;111:1700–3.
- [119] Mishchenko MI, Videen G, Babenko VA, Khlebtsov NG, Wriedt T. T-matrix theory of electromagnetic scattering by particles and its applications: a comprehensive reference database. *J Quant Spectrosc Radiat Transf* 2004;88:357–406.
- [120] Moffitt JR, Chemla YR, Smith SB, Bustamante C. Recent advances in optical tweezers. *Annu Rev Biochem* 2008;77:205–28.
- [121] Morse PM, Feshbach H. Methods of theoretical physics. New York: McGraw-Hill; 1953.
- [122] Neves AAR, Fontes A, Padilha LA, Rodriguez E, de Brito Cruz CH, Barbosa LC, et al. Exact partial wave expansion of optical beams with respect to an arbitrary origin. *Opt Lett* 2006;31(16):2477–9.
- [123] Nichols EF, Hull GF. A preliminary communication on the pressure of heat and light radiation. *Phys Rev* 1901;13(5):307–20.

- [124] Nichols EF, Hull GF. Pressure due to light and heat radiation. *Astrophys J* 1902;15:62–5.
- [125] Nieminen TA, Heckenberg NR, Rubinsztein-Dunlop H. Optical measurement of microscopic torques. *J Mod Opt* 2001;48:405–13.
- [126] Nieminen TA, Heckenberg NR, Rubinsztein-Dunlop H. Forces in optical tweezers with radially and azimuthally polarized trapping beams. *Opt Lett* 2008;33(2):122–4.
- [127] Nieminen TA, Loke VLY, Stilgoe AB, Heckenberg NR, Rubinsztein-Dunlop H. T-matrix method for modelling optical tweezers. *J Mod Opt* 2011;58:528–44.
- [128] Nieminen TA, Loke VLY, Stilgoe AB, Knoner G, Brańczyk AM, Heckenberg NR, et al. Optical tweezers computational toolbox. *J Opt A: Pure Appl Opt* 2007;9:S196–203.
- [129] Nieminen TA, Parkin S, Asavei T, Loke VLY, Heckenberg NR, Rubinsztein-Dunlop H. Optical vortex trapping and the dynamics of particle rotation. In: Andrews DL, editor. *Structured light and its applications*. San Diego: Academic Press; 2008. p. 195–236 [Chapter 8].
- [130] Nieminen TA, Rubinsztein-Dunlop H, Heckenberg NR. Calculation of the T-matrix: general considerations and application of the point-matching method. *J Quant Spectrosc Radiat Transf* 2003;79–80:1019–29.
- [131] Nieminen TA, Rubinsztein-Dunlop H, Heckenberg NR. Multipole expansion of strongly focussed laser beams. *J Quant Spectrosc Radiat Transf* 2003;79–80:1005–17.
- [132] Onofri F, Gréhan G, Gouesbet G. Electromagnetic scattering from a multilayered sphere located in an arbitrary beam. *Appl Opt* 1995;34:7113–24.
- [133] Padgett M, Allen L. Light with a twist in its tail. *Contemp Phys* 2000;41:275–85.
- [134] Padgett MJ, Allen L. The Poynting vector in Laguerre–Gaussian laser modes. *Opt Commun* 1995;121:36–40.
- [135] Penfield Jr. P, Haus HA. Electromagnetic force density. *Proc IEEE* 1966;54(2):328.
- [136] Peterman EJG, Gittes F, Schmidt CF. Laser-induced heating in optical traps. *Biophys J* 2003;84(2):1308–16.
- [137] Peterson B, Strom S. T-matrix formulation of electromagnetic scattering from multilayered scatterers. *Phys Rev D* 1974;10:2670–84.
- [138] Pfeifer RNC, Nieminen TA, Heckenberg NR, Rubinsztein-Dunlop H. Optical tweezers and paradoxes in electromagnetism. *J Opt* 2011;13(4):044017.
- [139] Phillips WD. Laser cooling and trapping of neutral atoms. *Rev Mod Phys* 1998;70:721–41.
- [140] Poynting JH. On the transfer of energy in the electromagnetic field. *Philos Trans R Soc Lond* 1884;175:343–61.
- [141] Qin J-Q, Wang X-L, Jia D, Chen J, Fan Y-X, Ding J, et al. FDTD approach to optical forces of tightly focused vector beams on metal particles. *Opt Express* 2009;17:8407–16.
- [142] Ren KF, Gréhan G, Gouesbet G. Radiation pressure forces exerted on a particle arbitrarily located in a Gaussian beam by using the generalized Lorenz–Mie theory, and associated resonance effects. *Opt Commun* 1994;108:343–54.
- [143] Robertson HP. Dynamical effects of radiation in the solar system. *Mon Not R Astron Soc* 1937;97(6):423–38.
- [144] Roosen G. La lévitation optique de sphères. *Can J Phys* 1979;57:1260–79.
- [145] Roosen G, Delaunay B, Imbert C. Étude de la pression de radiation exercée par un faisceau lumineux sur une sphère réfringente. *J Opt (Paris)* 1977;8(3):181–7 [Radiation pressure exerted by a light beam on refractive spheres: theoretical and experimental study].
- [146] Roosen G, Imbert C. Optical levitation by means of two horizontal laser beams: a theoretical and experimental study. *Phys Lett A* 1976;59:6–8.
- [147] Rubinsztein-Dunlop H, Nieminen TA, Friese MEJ, Heckenberg NR. Optical trapping of absorbing particles. *Adv Quantum Chem* 1998;30:469–92.
- [148] Siegman AE. *Lasers*. Oxford: Oxford University Press; 1986.
- [149] Simpson SH, Hanna S. Application of the discrete dipole approximation to optical trapping calculations of inhomogeneous and anisotropic particles. *Opt Express* 2011;19:16526–41.
- [150] Singer W, Nieminen TA, Gibson UJ, Heckenberg NR, Rubinsztein-Dunlop H. Orientation of optically trapped nonspherical birefringent particles. *Phys Rev E* 2006;73:021911.
- [151] Soper DE. *Classical field theory*. New York: Wiley; 1976.
- [152] Stein S. Addition theorems for spherical wave functions. *Q Appl Math* 1961;19(1):15–24.
- [153] Stilgoe AB, Heckenberg NR, Nieminen TA, Rubinsztein-Dunlop H. Phase-transition-like properties of double-beam optical tweezers. *Phys Rev Lett* 2011;107:248101.
- [154] Stilgoe AB, Mallon MJ, Cao Y, Nieminen TA, Rubinsztein-Dunlop H. Optical tweezers toolbox: better, faster, cheaper; choose all three. *Proc SPIE* 2012;8458:84582E.
- [155] Stilgoe AB, Nieminen TA, Knoner G, Heckenberg NR, Rubinsztein-Dunlop H. The effect of Mie resonances on trapping in optical tweezers. *Opt Express* 2008;16(19):15039–51.
- [156] Stout B, Rolly B, Fall M, Hazart J, Bonod N. Laser-particle interactions in shaped beams: beam power normalization. *J Quant Spectrosc Radiat Transf* 2013;126:31–7.
- [157] Taylor JM, Love GD. Multipole expansion of Bessel and Gaussian beams for Mie scattering calculations. *J Opt Soc Am A* 2009;26:278–82.
- [158] Taylor MA, Bowen WP. A computational tool to characterize particle tracking measurements in optical tweezers. *J Opt* 2013;15:085701.
- [159] Tough RJA. The transformation properties of vector multipole fields under a translation of coordinate origin. *J Phys A: Math General* 1977;10(7):1079–87.
- [160] Tsander FA. *Problems of flight by jet propulsion*. Jerusalem: Israel Program for Scientific Translations; 1964.
- [161] Umov NA. *Ableitung der Bewegungsgleichungen der Energie in kontinuierlichen Körpern*. *Z Math Phys* 1874;19:418–31.
- [162] van de Hulst HC. *Light scattering by small particles*. New York: Wiley; 1957.
- [163] van Enk SJ, Nienhuis G. Commutation rules and eigenvalues of spin and orbital angular momentum of radiation fields. *J Mod Opt* 1994;41(5):963–77.
- [164] Videen G. Light scattering from a sphere near a plane interface. In: Moreno F, González F, editors. *Light scattering from microstructures*. Lecture notes in physics, vol. 534. Berlin: Springer-Verlag; 2000. p. 81–96 [Chapter 5].
- [165] Visscher K, Brakenhoff GJ. Theoretical study of optically induced forces on spherical particles in a single beam trap I: Rayleigh scatterers. *Optik* 1992;89:174–80.
- [166] Visscher K, Brakenhoff GJ. Theoretical study of optically induced forces on spherical particles in a single beam trap II: Mie scatterers. *Optik* 1992;90:57–60.
- [167] Wang JJ, Gouesbet G, Han YP. Transformations of spherical beam shape coefficients in generalized Lorenz–Mie theories through rotations of coordinate systems: II. Axisymmetric beams. *Opt Commun* 2010;283:3226–34.
- [168] Waterman PC. Matrix formulation of electromagnetic scattering. *Proc IEEE* 1965;53(8):805–12.
- [169] Waterman PC. Symmetry, unitarity, and geometry in electromagnetic scattering. *Phys Rev D* 1971;3:825–39.
- [170] White CA, Head-Gordon M. Rotating around the quartic angular momentum barrier in fast multipole method calculations. *J Chem Phys* 1996;105(12):5061–7.
- [171] White DA. Numerical modeling of optical gradient traps using the vector finite element method. *J Comput Phys* 2000;159:13–37.
- [172] White DA. Vector finite element modeling of optical tweezers. *Comput Phys Commun* 2000;128:558–64.
- [173] Wright WH, Sonek GJ, Berns MW. Parametric study of the forces on microspheres held by optical tweezers. *Appl Opt* 1994;33(9):1735–48.
- [174] Wu ZS, Guo LX, Ren KF, Gouesbet G, Gréhan G. Improved algorithm for electromagnetic scattering of plane waves and shaped beams by multilayered spheres. *Appl Opt* 1997;36:5188–98.
- [175] Zambrini R, Barnett SM. Local transfer of optical angular momentum to matter. *J Mod Opt* 2005;52(8):1045–52.
- [176] Zhang H, Liu K-K. Optical tweezers for single cells. *J R Soc Interface* 2008;5(24):671–90.